ADVANCED FUNCTIONAL MATERIALS
www.afm-journal.de

A Review of Perovskites Solar Cell Stability

Rui Wang, Muhammad Mujahid, Yu Duan, Zhao-Kui Wang, Jingjing Xue, and Yang Yang**

In this review, the factors influencing the power conversion efficiency (PCE) of perovskite solar cells (PSCs) is emphasized. The PCE of PSCs has remarkably increased from 3.8% to 23.7%, but on the other hand, poor stability is one of the main facets that creates a huge barrier in the commercialization of PSCs. Herein, a concise overview of the current efforts to enhance the stability of PSCs is provided; moreover, the degradation causes and mechanisms are summarized. The strategies to improve device stability are portrayed in terms of structural effects, a photoactive layer, hole- and electron-transporting layers, electrode materials, and device encapsulation. Last but not least, the economic feasibility of PSCs is also vividly discussed.

1. Introduction

Global energy consumption has been gradually increasing. Limited sources of fossil fuels are demanding the research on sustainable and renewable energy resources. The conversion of sunlight into electricity is one of the most promising studies to meet the increasing energy demands for future generations without the negative impact of the global climate. Solar cell technology provides an ecofriendly and renewable energy route to convert photon energy into electricity directly.[1] Now a days scientist intends to design photovoltaic devices with high efficiency, low cost, and large-scale fabrication but unfortunately did not succeed yet. However, the efficient establishment of solar cell technology on a global scale requires an efficient improvement concerning materials and devices to reduce the fabrication cost and increase the power conversion efficiency.[1b]

R. Wang, Prof. Y. Duan, Prof. Z.-K. Wang, J. Xue, Prof. Y. Yang
Department of Materials Science and Engineering
University of California at Los Angeles
Los Angeles, CA 90095, USA
E-mail: duanyu@jlu.edu.cn; yangy@ucla.edu
M. Mujahid, Prof. Y. Duan
State Key Laboratory on Integrated Optoelectronics
College of Electronic Science and Engineering
Jilin University
Changchun 130012, China
Prof. Z.-K. Wang
Jiangsu Key Laboratory for Carbon-Based Functional Materials & Devices
Institute of Functional Nano & Soft Materials (FUNSOM)
Soochow University
Suzhou 215123, China
The ORCID identification number(s) for the author(s) of this article can be found under https://doi.org/10.1002/adfm.201808843.

DOI: 10.1002/adfm.201808843

Perovskite solar cells (PSCs) have recently been universally promoted as an economically and environmentally feasible renewable technology option to traditional solar cell technologies for addressing global challenges in the area of energy generation and climate change.[2] The organic–inorganic perovskite with an ABX_3 structure where A is cesium (Cs), methyl ammonium (MA), or formamidinium (FA); B is Pb or Sn; and X is Cl, Br, or I, have recently emerged as an intriguing class of semiconductors.[3] There are various techniques in which perovskites can be processed such as spray coating, a nozzle is used to disperse tiny liquid droplets onto substrates the perovskite layer can also be deposited by ultrasonic spraying.[4] Dip coating, a nonconventional method to create the meniscus edge, is pulling a substrate out of a precursor ink and sheering a cover plate over the deposition substrate,[5] two-step deposition[6] in which the lead halide thin film is first deposited then converted to the perovskite by reaction with organic halide salts.[5a] Chemical vapor deposition[7] (CVD) has been used to deposit $FAPbI_3$ thin films on 5 cm × 5 cm substrates and to fabricate 12 cm^2 modules with a PCE of 9%.[8] Ink-jet printing nozzles are used to disperse the precursor ink, with fine control of the droplet size and trajectory. Small-area PSCs (0.04 cm^2) have been fabricated using inkjet printing.[9] PSCs fabricated by blade coating has demonstrated PCEs >19%.[10] And screen printing method has good patterning ability with a lateral resolution of 75–100 μm.[11] Perovskites have exceptional properties such as absorption over a wide spectrum,[12] a direct bandgap,[13] charge carrier diffusion lengths in the micrometer range,[14] and defect tolerance.[15] An unprecedented rise in the efficiency from 3.8% to 23.7% was achieved in only a few years, which extremely outperformed many proven commercial photovoltaic technologies, e.g., Si, GaAs, and CdTe-based solar cells.[16]

Massive technologies have been developed to improve the performance of the PSCs, including solvent engineering, interfacial engineering, bandgap engineering, and etc.[17] Reported by Grätzel group in 1991, dye-sensitized solar cell (DSSC) has been paid intensive attention in the passing decades. Up to now the certified highest PCE of DSSC has reached 11.9%[18] presenting excellent market competitiveness and commercial prospect. In 1998, Grätzel and co-workers from Switzerland first reported a hole-transporting material (HTM), 2,2,7,7-tetrakis (*N,N*-di-methoxy-phenyl amine)-9, 9-spirobifluorene (spiro-OMeTAD), to replace the conventional liquid-state electrolyte and developed a solid-state DSSC (ss-DSSC).[19] From

1998 to 2011, the PCE of ss-DSSC fast increased from 0.74% to 7.2%, but still much lower than that obtained by liquid-state electrolyte based DSSCs.[20] In late 2012, a remarkable breakthrough was made by using $CH_3NH_3PbI_3$ ($MAPbI_3$) perovskite nanocrystals as the light absorber to fabricate a solid-state mesoporous perovskite solar Cell (MPSC) with a PCE of up to 9.7%.[21] Etgar et al. fabricated an efficient HTM-free TiO_2/$MAPbI_3$/Au solar cell with an efficiency of 10.49%.[22] After that Snaith's group reported a planar thin-film architecture PSC with a PCE of 12.3%.[23] In 2014, the PCE increased to a certified 17.9% and then 20.1%.[24] And a low temperature and solution processable ionic liquid, $[BMIM]BF_4$, is recently utilized to act as an effective electron modification layer and a protective layer for fabricating high-performance indoor and outdoor PSCs. The device delivered an impressive PCE of 19.30% at 1 sun illumination, and a record indoor PCE of 35.20% under a fluorescent lamp with 1000 lux, which was the highest value reported so far for indoor PSCs.[25]

At present, the most challenging issue in perovskite solar cells is the long-term stability, which must be cleared up before putting it into practical applications. As we know that the stability of perovskite solar cells upon the severe environment, e.g., thermal treatment, light illumination, humidity, etc., appears to be the bottleneck that impedes their further commercialized.[26] Among them, the humidity is demonstrated to be one of the possible causes for the degradation of perovskites.[27] Zhou et al. reported that exposure to a low level of humidity (RH ≈ 30%) during solar cell fabrication was capable of controlling the perovskite crystal formation and aided them in enhancing the PCE to 19.3%.[28] Bass et al. reported how humidity could speed up the perovskite crystallization.[29] These studies suggest that rationally controlled amount of H_2O could assist the grain growth of perovskite then result in the film with high quality, carrier mobility and lifetime film, though the excess moisture will damage the crystallinity once the films are prepared.[30] To entirely keep away from any ambient exposure before finishing the device, about all groups performed the perovskite deposition in a dry atmosphere and endeavor to avoid exposure to humidity. Generally, PSCs have two architectures, i) mesostructured device, and ii) planar device. In a mesostructured device, the perovskite is used to sensitize the mesoporous titania (TiO_2) layer.[31] Whereas the planar device has a comparatively simpler structure and gives better cell performance. Gradual improvement of the perovskite film quality improved the overall cell efficiency.[31,32]

2. Structural Influence on the Stability of PSCs

2.1. Structure of Perovskite Devices

PSCs consist of active perovskite layer that is sandwiched between electron-transporting layer (ETL) and hole-transporting layer (HTL). If the light goes through ETL, transparent conducting layer exist in front of ETL then it is known as n–i–p structure. The opposite one should be p–i–n as shown in **Figure 1**a,b. Mesoscopic and planar these are two basic structures; typically mesoscopic structure has an n–i–p configuration: compact ETL/mesoporous ETL/perovskite/HTL/electrode (Figure 1c). The planar type PSCs are further divided into two band configurations: n–i–p planar and p–i–n planar (Figure 1d,e).[33] The n–i–p structure usually involves depositing

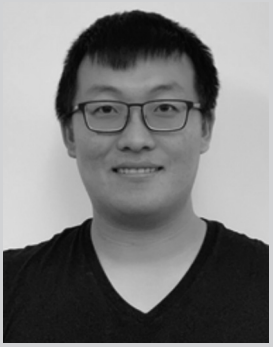

Rui Wang received his bachelor degree (2015) and master degree (2016) in materials science and engineering from Jilin University and University of California, Berkeley, respectively. He is currently a PhD student in the Department of Materials Science and Engineering at University of California, Los Angeles under the supervision of Prof. Yang Yang. His research focuses on developing highly efficient and stable perovskite optoelectrical devices and organic photovoltaics.

Yu Duan received his Ph.D. in microelectronics and solid-state electronics from the Jilin University of 2006 under the supervision of Prof. Shiyong Liu. He received his postdoctoral training in the National Nanotechnology Laboratory of CNR-INFM (2007–2010) working under Prof. Giuseppe Gigli. He is presently a Professor at the State Key Laboratory on Integrated Optoelectronics, College of Electronic Science and Engineering, Jilin University.

Yang Yang holds a B.S. in physics from the National Cheng-Kung University in Taiwan in 1982, and he received his M.S. and Ph.D. in physics and applied physics from the University of Massachusetts, Lowell in 1988 and 1992, respectively. Before he joined UCLA in 1997, he served on the research staff of UNIAX (now DuPont Display) in Santa Barbara from 1992 to 1996. Yang is now the Carol and Lawrence E. Tannas Jr. Endowed Chair Professor of Materials Science and Engineering at UCLA. He is a materials physicist with expertise in the fields of organic electronics, organic/inorganic interface engineering, and the development and fabrication of related devices, such as photovoltaic cells, LEDs, and memory devices.

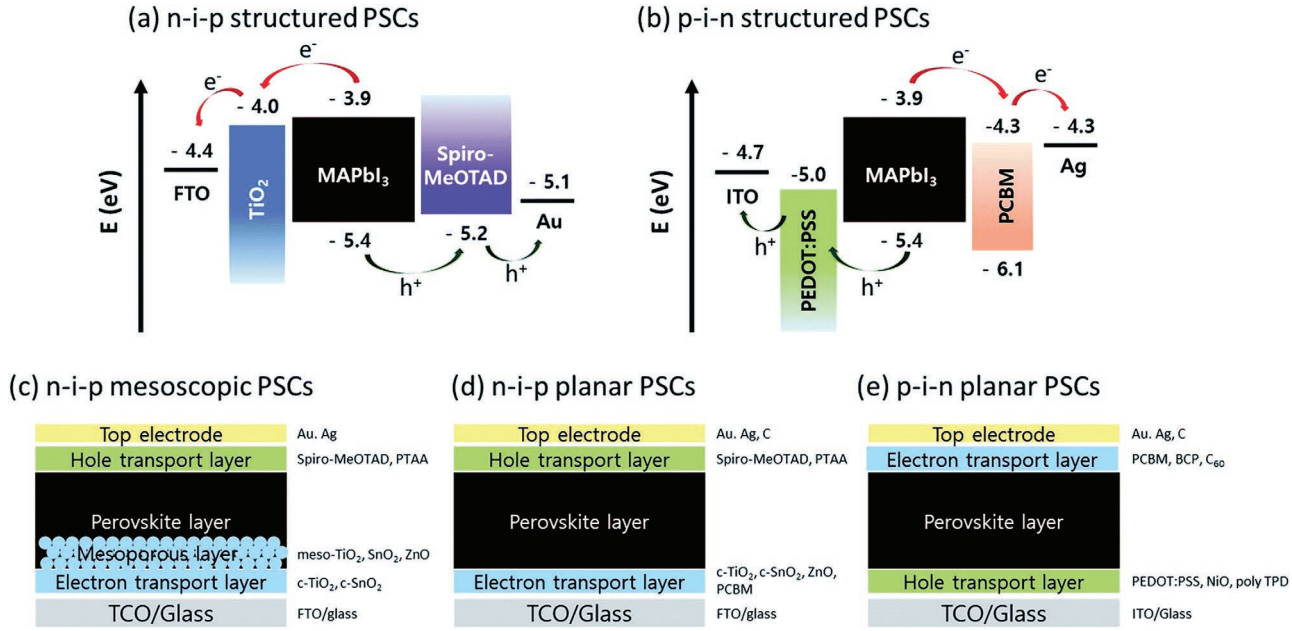

Figure 1. Energy band diagram of typical a) n–i–p and b) p–i–n structured PSCs; device structures of c) n–i–p mesoscopic, d) n–i–p planar, and e) p–i–n planar PSCs. Reproduced with permission.[33] Copyright 2018, Royal Society of Chemistry.

the perovskite material onto transparent substrates covered with a compact TiO_2 layer and an optional mesoporous TiO_2 (or Al_2O_3) scaffold layer.[34] The p–i–n structure, which involves depositing the perovskite material onto transparent substrates which are covered with an HTL, such as the poly(3,4-ethylene dioxythiophene):polystyrene sulfonic acid (PEDOT:PSS).[35] So far, PSCs based on both mesoporous and planar structure exhibit high performance and stability, however, the comparison of the advantages of two different strucutres in stability is still under debate.[36]

2.2. Mesoporous Perovskite Solar Cells

Recently, a new generation of photovoltaic converters, mesoporous solar cell[37] has attracted more consideration due to their low material cost, simple fabrication process, high energy conversion efficiencies,[38] like dye-sensitized solar cell,[38c] and mesoporous perovskite solar cell.[5a,21,39] PCE up to 9.7% has been achieved by using $CH_3NH_3PbI_3$ ($MAPbI_3$) perovskite nanocrystals as the light absorber to fabricate a solid-state MPSC.[21] After that the research focuses on solid-state MSCs began to transfer from DSSCs to MPSCs.[32a,40] In an MPSC, a compact layer is usually deposited on fluorine doped tin oxide (FTO) layer, which usually extracts electrons and block holes. Three strategies are broadly used for depositing the TiO_2 layer: 1) Spin-coating the colloidal dispersion of TiO_2 nanoparticles followed by a thermal treatment (titanium source: $TiCl_4$,[41] titanium isopropoxide,[42] tetra-*n*-butyl-titanate;[43] 2) spin-coating titanium precursor solutions followed by a thermal treatment (titanium source: $TiCl_4$,[44] titanium isopropoxide,[23] titanium diisopropoxide bis(acetylacetonate)[12]); 3) spray pyrolysis deposition (titanium source: titanium diisopropoxide bis(acetylacetonate)[18]).[45] Low-temperature sintering approaches to prepare an effective TiO_2 layer in perovskite solar cells have been recently reported.[44,46]A mesoporous layer deposited on top of the compact layer[47] by spin coating, screen printing,[48] magnetron sputtering,[49] or electrospinning.[50] The structure and thickness of the mesoporous layer impact on device performance. Decreasing the thickness of the mp-TiO_2 layer can help the pore-filling process and thus result in improved efficiency.[51] The mesoporous layer also offers to suppress hysteresis.[52] Miyasaka and co-workers improved the efficiency of such perovskite-sensitized solar cell to 3.8% by replacing bromine with iodine ($MAPbI_3$).[53] Park and Grätzel's group reported that employment of solid-state organic HTM not only solved the problem that perovskites may dissolve in the liquid-state electrolyte, which significantly improved the stability of the device but also boosted the reported efficiency of solid-state MSCs to 9.7%.[21] Nazeeruddin and co-workers introduced a layered sandwich-type structure in which 3D nanocomposites of mesoporous (mp)-TiO_2, with methylammonium lead triiodide $CH_3NH_3PbI_3$ as a light harvester and polymeric HTMs were used and got the efficiency of 12%.[54] Seok's group further improved efficiency to 12.3% with the same structure but mixed halide $CH_3NH_3PbI_{3-x}Br_x$ perovskites.[40b] However, Lee et al. reported a PSC comprised of mesoporous Al_2O_3 instead of TiO_2, demonstrating that the Al_2O_3 merely acted as a scaffold layer without injection of photoexcited electrons Small perturbation transient photo current decay measurements revealed that charge collection was ten times faster in the Al_2O_3-based cell than in the TiO_2-based one, the electron diffusion is faster through the perovskite than in the n-type TiO_2.[9b] Using a thin Al_2O_3 film ≈80 nm at low temperature <150 °C, Snaith and co-workers fabricated a flat junction thin film solar cell with a thick perovskite capping layer on the top of scaffold and improved the FTO/bl-TiO_2/mp-Al_2O_3/$MAPbI_{3-x}Cl_x$/spiro-OMeTAD/Ag-based efficiency to 12.3% (J_{sc} = 18 mA cm^{-2}, V_{oc} = 1.02 V, and

FF = 0.67).[23] Nanostructured ZnO is a viable n-type alternative scaffold to mp-TiO_2 for perovskite solar cells because it offers not only higher electron mobility but also bandgap of ≈3.37 eV at 25 °C. Mahmood and co-workers fabricated a mesoporous ZnO film (≈440 nm) using the electrospraying method, a PCE of 10.8% was achieved, with a J_{sc} of 16 mA cm^{-2}, V_{oc} of 1.01 V, and FF of 0.67.[55] When the ZnO film was doped with Al, the device yielded a higher PCE of 12%, with V_{oc} = 1.045 V, FF = 0.76.[56] Kim et al. reported that solid-state mesoscopic heterojunction PSCs shows the stability of encapsulated devices stored for over 500 h in air at room temperature.[21] The focus has been recently shifted primarily towards tuning the perovskite composition given obtaining a more stable active layer.[57] The triple cation based PSCs fabricated by Saliba et al. have demonstrated stability for 250 h under a nitrogen atmosphere, but the stability in the presence of humidity remains unknown.[58]

2.3. Planar Perovskite Solar Cell (n–i–p)

Planar perovskite solar cells (PPSCs) have been widely studied due to their unique advantages such as low cost, easy processing, and low-temperature process.[59] PPSCs can be fabricated using either a normal structure or inverted structure (Figure 1d,e). The normal structure is similar to that of MPSCs, except that it does not utilize mesoporous materials.[60] Inverted structures typically use organic-semiconductors as both HTL and ETL[17d,61] such as [6,6]-phenyl-C61-butyric acid methyl ester (PCBM), indene-C60 bisadduct (ICBA), C_{60}-SAMorpolyelectrolytepoly[(9,9-bis(3′-(*N,N*-dimethylamino) propyl)-2,7-fluorene)-alt-2,7-(9,9-dioctylfluorene)] (PFN) and form the basis of PPSCs.[45,60] In PPSCs, each layer has an important influence on the device's performance.[62] Many strategies have been adopted to optimize the performance of planar p–i–n PSCs such as perovskite crystalline regulation,[63] design of new perovskite component,[64] geomorphology control,[65] and modification of the charge carriers transport layers.[66] Generally, PEDOT:PSS is fabricated upon the transparent anode to realize smooth surface and regulate the energy level between the perovskite layer and electrode. The insulated PSS restricts the charge transport within the PEDOT:PSS layer, which leads to accumulation of charge carrier at the interfaces to reduce the performance of PSCs.[67] Yu et al. reported that a 31% improvement in the device average PCE from 11.14% to 14.61% with negligible hysteresis. They imply that ammonium metatungstate hydrate (AMH) doped PEDOT:PSS has the potential to be an excellent HTL and a step toward achieving highly efficient and long stability PSCs.[68] Briseno et al. observed not only enhanced efficiency but also improved long-term stability by a simple solution processed interfacial modification method using self-assembled monolayer (SAM). Interfacial modifications were carried out using a new series of fluorine-functionalized boronic acid SAMs. 2F-SAMs modification exhibits 16% efficiency and long-term stability also provide a permanent ITO work function modification and prevents the degradation of ITO because of the acidic effect of PEDOT:PSS.[69]

Planar devices employing atomic layer deposited (ALD) SnO_2 as the electron selective layer yielding efficiency of 19.5%. SnO_2 was shown to exhibit well-aligned conduction bands of the perovskite and SnO_2 materials in a planar configuration.[70] Correa-Baena and co-workers reported that low-temperature planar PSCs are suited for large-scale manufacturing.[71] Proposed a simple, solution-processed technological approach for depositing SnO_2 layers, reaching a PCE close to 21%, which is much better efficiency for any planar configuration. As for as the stability of the device is a concern, the devices showed a final PCE of 20.7% after aging and several hours of dark, dry air storage, being higher than the initial pre-aged measurement of 20.4%.[71] Zhu and co-workers published a champion power conversion efficiency of 21.11% with a stabilized power output of 20.83% and negligible hysteresis.[70b] The planar device architecture is used because it is inherently more compatible with flexible and tandem applications. Currently, planar PSCs show relatively high PCEs > 20% and up to 21.4%.[74] That is slightly lower than mesoporous-containing perovskites.[75] Planar PSCs do not reach world records yet; researchers are less willing to switch from meso to planar, even though it is industrially more preferable.[76]

2.4. Planar Perovskite Solar Cell (p–i–n)

Inverted structure devices have exhibited many advantages such as easy fabrication process, negligible hysteresis, and high stability.[77] Inverted PSCs have great potential for application in flexible and high-performance photovoltaic devices.[78] PEDOT:PSS has been widely used as a hole-transporting material for inverted PSCs due to its higher conductivity and good transparency in the visible range.[79] PEDOT:PSS is hydrophilic and can easily absorb water from the surrounding environment.[59c] Many inverted PSCs are constructed with the PEDOT:PSS/perovskite/PCBM heterojunction configuration (PEDOT = poly(3,4-ethylene dioxythiophene) and PSS = polystyrene sulfonate).[80] Inverted structures typically use organic-semiconductors as both HTL (e.g., PEDOT:PSS)[17d,61] and ETL (e.g., PCBM, ICBA, C_{60}-SAM or polyelectrolyte poly[(9,9-bis(3′-(*N,N*-dimethylamino)propyl)-2,7-fluorene)-alt-2,7- (9,9-dioctylfluorene)] (PFN)), and form the basis of PPSCs devices.[45] The first inverted planar PSCs were originated from the concept of organic photovoltaics where PEDOT:PSS was used as hole-transporting material and PCBM as electron-transporting material.[81] Heo et al. compared the inverted structure (ITO/PEDOT: PSS/$MAPbI_3$/PCBM/Au) with a normal structure (FTO/TiO_2/$MAPbI_3$/PTAA/Au) and found that the inverted structure had a higher efficiency.[82] Wang et al. used modified PEDOT:PSS HTL yielded an enhanced PCE of 15.7% with an enlarged V_{oc} of 1.06 V and improved long-term stability.[83] The basic PEDOT:PSS can suppress the indium diffusion into the active layer, which can maintain 75% of its original PCE and 95% of original V_{oc} after 14 d storage in ambient condition with a controlled 20% relative humidity.

Highly efficient PSCs can be obtained by doping sodium chloride (NaCl) into PEDOT:PSS solution with an impressive FF and V_{oc}.[84] NaCl influences not only the electrical properties of PEDOT:PSS but also impact the nucleation and growth of perovskite on top of PEDOT:PSS. At the optimal NaCl doping concentration of 5 mg mL^{-1}, a high V_{oc} and FF of 1.08 eV

and 80.0% are achieved, resulting in a PCE of 18.2% in the $MAPbI_{3-x}Cl_x$-based PSCs. Huang et al. get enhanced long-term stability as compared to PEDOT:PSS under unencapsulated conditions by DA-PEDOT:PSS-based PSC.[67b] The PCE and J_{sc} retained 85.4% and 89.2% of their original values. Even after 28 d of aging as compared to 60.4% and 59.3%, respectively, These results indicate a bright future for dopamine-doped PEDOT:PSS due to its promising properties. Yang et al. demonstrated a high-performance planar heterojunction PSC with a PCE of 14.82%.[83] Chiang et al. achieved the best PCE of 16.31% by inserting the Ca between the PCBM and electrode.[73] Im and co-workers fabricated hysteresis-less planar $MAPbI_3$ perovskite hybrid solar cells with 18.1% power conversion efficiency by constructing the inverted device architecture of ITO/PEDOT: PSS/$MAPbI_3$/PCBM/Au.[80] The better efficiency, stability, and lower *J–V* hysteresis of the inverted cells were obtained. However, the PEDOT: PSS/ITO interface is recognized as one of the major factors for deteriorating the performance of the PSCs.[67b,85] Some employed other materials except PEDOT:PSS, as another approach if a certain material whose work function is in between PEDOT:PSS and ITO, it will enhance the stability and PCE.[67b,86]

Recently, graphene oxide flakes have been inserted between PEDOT:PSS and ITO to improve the durability and efficiency of the PSCs. Besides, graphene has various advantages such as high visible light transmittance, easy work function control, excellent chemical stability, and excellent gas barrier properties.[87] As for as the stability of the device is concern carbon derivatives such as graphene,[88] graphene oxide,[89] reduced graphene oxides[90] are very popular. Kim et al. employ gold (III) chloride ($AuCl_3$)-doped graphene (GR) as a protecting layer between PEDOT:PSS and ITO for improving the efficiency and durability of the PSCs.[91] $AuCl_3$-GR PSC shows maximum PCEs of 15.77% and 15.90% for forwarding/reverse condition, respectively. Besides, it showed a significant improvement in the durability by maintaining 67% of its original PCE even after 30 d in the unencapsulated state. Chowdhury et al. reported reduced graphene oxide (r-GO)/copper (I) thiocyanate (CuSCN) as an efficient bilayer HTL for low temperature processed inverted planar PSCs, showed PCE of up to 14.28% with an improved light soaking stability up to 100 h.[92] Yang et al. proposed thermal rGO as one of the most promising materials for application in planar inverted PSCs.[89] Yeo et al. suggested the use of fluorinated reduced graphene oxide (MFGO) as an alternative HTL, instead of PEDOT:PSS.[93] Zhou et al. proposed the incorporation of a bilayer composed of rGO and PTAA as the HTL in planar inverted MAPbI3 PSCs.[94]

Fullerene-based ETLs are most popular in inverted PSCs,[95] due to their simple device architecture, low-temperature preparation process, and negligible hysteric behavior.[78b,96] Huang and co-workers introduced PFN-2TNDI as an alternative to PCBM as the ETL in inverted Pero-SCs.[97] The PFN-2TNDI-based devices improved the efficiency (16.7%) and long-term stability. Tian et al. reported that the improved efficiency and stability of PC61BEH-based devices could be attributed to the presence of the branched group that enhances solubility, improves film morphology and increases both passivation and electron extraction ability.[98] Park and co-worker designed and synthesized a novel NDI-based polymeric ETL to replace PCBM in an inverted PSC.[99] The highest photovoltaic performance with a PCE of 17.0% and negligible hysteresis in the field of polymeric ETLs has been delivered. This method improves both the light-induced and long-term stability of these devices under ambient conditions.

Some n-type semiconductor materials have been applied to the ETL such as TiO_2,[100] ZnO, SnO_2, and Zn_2SnO_4,[100,101] these materials require high-temperature annealing in practical applications.[72b] This process will make the light absorption layer degrade quickly and destroy the integrity of light absorption in inverted structure. To overcome this problem, cadmium sulfide (CdS) nanoparticles are the best option as the electron transport layer in the inverted structure. Jia et al. reported that the PSC with a CdS ETL shows a negligible hysteresis and better stability than that of the PSC assembled with a PCBM ETL.[102] Liu et al. developed a novel and highly efficient inverted PSC with thermally evaporated C_{60} and CuPc as ETL and HTL, respectively.[103] A stabilized PCE output of 16.38% is obtained measured at the maximum power point for over 1000 s showing improved operation stability. Carbon nanomaterials featuring low cost, excellent electrical property, and outstanding stability are becoming promising candidates for metallic electrodes and have been widely used in n–i–p PSCs. CNT films used as back contact have been reported in conventional PSCs but rarely in inverted PSCs.[104] Zhou et al. employed a novel poly ethyleneimine (PEI)-modified cross-stacked super-aligned carbon nanotube (CSCNT) film in the inverted planar PSCs.[105] CSCNT:PEI-based inverted PSCs show superior durability. Remaining over 85% of the initial PCE after 500 h aging under various conditions, including long-term air exposure, thermal, and humid treatment.

3. Instability of Phtotoactive Layer of PSCs

PCSs have recently attracted much attention due to their high PCE, cheap starting material, and ease of fabrication.[106] However, device stability has still been a severe hurdle toward commercialization of perovskite-based solar cells. The instability of the device comes mostly from the degradation of the perovskite materials. the instability has been linked to the organometallic absorber toward humidity,[108] and their overall poor long-term thermal stability.[109] Many attempts have been made to achieve better stability of PSCs, such as 2D perovskite structure designing,[110] cation engineering,[111] and an additive in the hole and electron transfer layer was used to enhance the stability of the PCSs.[112] Solving instability problem of perovskite material is the critical strategy to upgrade the long-term stability.

3.1. Moisture Instability

The degradation of PSCs in a humid environment is a challenging issue. Among different factors, moisture has been considered as one of the biggest challenges. The moisture instability originates due to the hygroscopic nature of amine salt.[113] Both $MAPbI_{3-x}Cl_x$ and $MAPbI_3$ endure similar moisture assisted degradation process in which the methylamine group is lost via sublimation and PbI_2 is formed.[114] The highly

hydrophilic properties of perovskite could lead to the materials to readily absorb water from the surrounding environment and induce the formation of hydrate products similar to $(CH_3NH_3)_4PbI_6.2H_2O$.[27] Previous work reported that PCSs are severely affected due to moisture and oxygen environmental sensitivity since degradation of perovskite by hydrolysis reaction and represented by following chemical equations.

$$CH_3NH_3PbI_3(s) \leftrightarrow PbI_2(s) + CH_3NH_3I(aq) \quad (1)$$

$$CH_3NH_3I(aq) \leftrightarrow CH_3NH_2(aq) + HI(aq) \quad (2)$$

$$4HI(aq) + O_2(g) \leftrightarrow 2I_2(s) + 2H_2O(I) \quad (3)$$

$$2HI(aq) \leftrightarrow H_2(g) + I_2(s) \quad (4)$$

The hydrogen bond between organic and inorganic units in a perovskite, it attributes to the structural ability, and it is strongly affected by the high polarity of a water molecule.[115] Previous works reported that the presence of mesostructured TiO_2 could be helpful for device stability and a device without mp-TiO_2 exhibit profound sensitivity to ambient conditions.[61b]

Efforts have been dedicated to developing the moisture tolerance of perovskite materials without degradation of their optoelectronic properties.[116] It is contrary to the thought that water or moisture is harmful to the fabrication of perovskite solar cells. Bass et al. reported better film formation of $MAPbI_3$ and $MAPbBr_3$ while they are spin-coated in the surrounding of air at 58.2% RH.[29] Snaith group reported that the optimal RH of 50% produces a PCE of more than 14% because of the elimination excess of MA^+,[117] the damage of $MAPbI_3$ by water vapor is reversible.[118] This behavior is thought to be due to reversible infiltration of the perovskite lattice during production and postproduction.[119]

In recent years, 2D PSCs have begun to gain attention because of their better stability.[57a,120] Cao et al. studied 2D homologous perovskites $(CH_3(CH_2)_3NH_3)_2(CH_3NH_3)_{n-1}Pb_nI_{3n+1}$ solar cells.[121] Recently, Tsai et al. prepared mixed-dimensional (MD) perovskites $(CH_3(CH_2)_3NH_3)_2(MA)_{n-1}Pb_nI_{3n+1}$ (n = 3,4), which shows a PCE of 12.52% and high light and stability.[122] Organic ammonium salt provides good self-assembly and film reforming properties. The combination of the inorganic framework and different ammonium salt may produce new performances in optical, electrical, and magnetic by changing organic and inorganic components.[123] Although there are many reports about the high stability of 2D perovskites.[120–122] Dai and co-workers reported that $(C_6H_5CH_2NH_3)_2(FA)_8Pb_9I_{28}$ quasi-2D perovskite film and the device display high stability in a moist environment. After exposure to RH 80% air for 500 h, the $(C_6H_5CH_2NH_3)_2(FA)_8Pb_9I_{28}$ film only slightly decomposes, and the device maintains 80% of its starting PCE.[124] They also suggest that the hydrophobicity of different ammonium salts can determine moisture resistance of 2D perovskite materials.[124] Adding a small amount of 2D perovskite into 3D perovskite improve not only moisture stability but also suppress nonradioactive recombination via passivating the surface defect and/or bulk tarps of 3D perovskite.[125] Also, negligible hysteresis can also be achieved by grain preferred orientation growth engineering,[122] and in situ nonstoichiometric precursor engineering.[126] According to the report on $FA_xPEA_{1-x}PbI_3$ used for inverted PSC showing a PCE of 17.7%, bulky organic cations can terminate perovskite lattice and thereby lead to the quantum well (QW) structure. A bulky organic cation can control the number of inorganic perovskite layers (width of QW).[127] The experimental results give important insight into the design of 2D/3D mixed perovskite to have a high carrier transport with less chance of recombination. Wang et al. incorporated BA into $FA_{0.83}Cs_{0.17}Pb(I_yBr_{1-y})_3$ 3D perovskite to produce 2D–3D heterostructured BA–Cs–FA lead halide perovskite for normal planar PSCs. 2D platelets were formed perpendicularly, and these could drive the vertical growth of 3D perovskite. Grain growth perpendicular to the substrate is expected to be favorable for charge transport, accompanied by longer charge diffusion length and lifetime as proved by significantly increased PL studies.[125c] 1D–3D hybrid perovskite materials were also proposed for the improvement of stability, where (1H-pyrazole-1-yr)pyridine (PZPY) was introduced into 3D $Cs_{0.04}MA_{0.16}FA_{0.8}PbI_{0.85}Br_{0.15}$ perovskite.[128]

It is found that 2D perovskites with general formula $(RNH_3)_2A_{n-1}M_nX_{3n+1}$ had appealing environmental stability.[129] Actually, 2D perovskites are derived from the archetypal AMX_3 3D structure by inserting bulky organic cations between the atomic layers. The hydrophobic nature of the organic spaces and relatively stable structure of 2D perovskite improve the stability of PSCs. 2D $(ZnPc)_{0.5}MA_{n-1}Pb_nI_{3n+1}$ was successfully constructed within the GBs of $MAPbI_3$ film achieving a GBs suture for passivating the defects in GBs.[130] The moisture stabilities of the PSCs were tested in air at room temperature with humidity of about 45% as shown in **Figure 2**. The modified perovskite retained over 95% of its original efficiency after 2000 h. In contrast, the device with pure perovskite film first exhibited a fast degradation rate by remaining only <65% of the initial efficiency under the same conditions, and the best efficiency was improved up to 20.3%.[130] Peng and co-workers reported that the synthesized PCBM/Al_2O_3– ZnO dramatically improves the stability of $CH_3NH_3PbI_3$ against the ambiance and even against liquid water.[131]

The effects of moisture on $CH_3NH_3PbI_3$ is of great interest because of its role in the degradation of perovskite solar cell

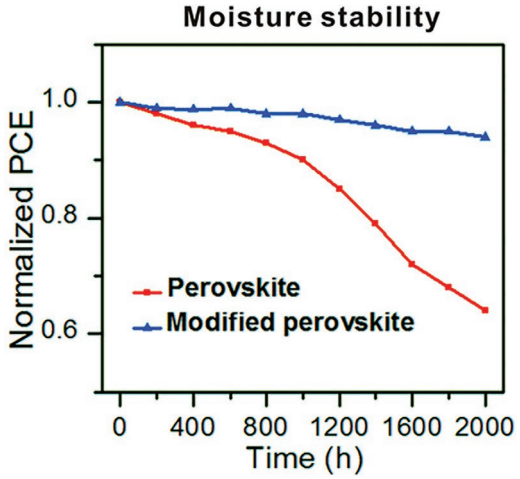

Figure 2. Moisture stability measured with a humidity of 45%. Reproduced with permission.[130] Copyright 2018, American Chemical Society.

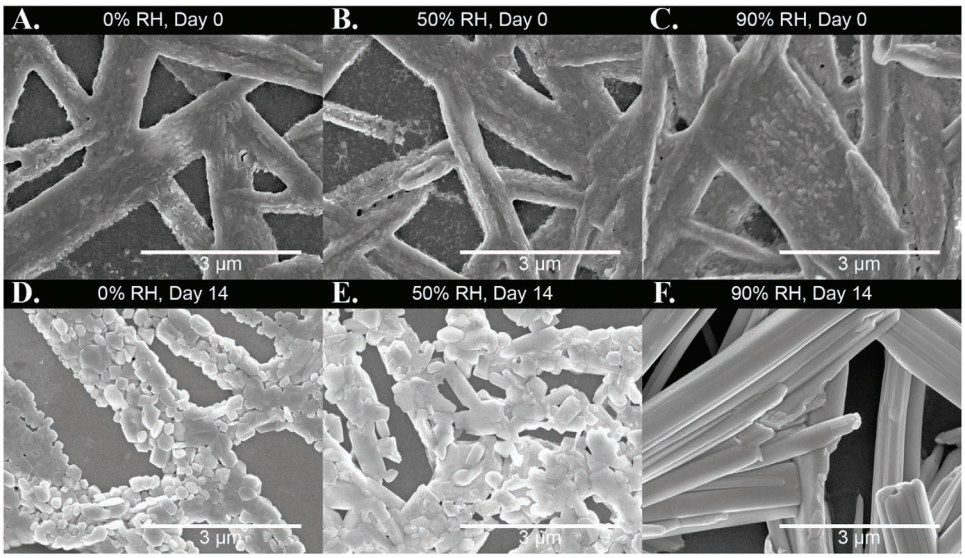

Figure 3. Top-down scanning electron micrographs of films stored in 0%, 50%, and 90%, RH for 14 d. Reproduced with permission.[27] Copyright 2015, American Chemical Society.

performance.[40b,132] To avoid exposure to humidity during solar cell fabrication, nearly all groups carry out perovskite deposition in a dry atmosphere and take pains to avoid exposure to humidity following device fabrication. Smith et al. showed that moisture stability could be improved by substituting $C_6H_5(CH_2)_2NH_3$ for CH_3NH_3I.[57a] Zhou et al. investigated that exposure to a low level of surrounding humidity (30% RH) during solar cell fabrication process, controlled the perovskite crystal formation, assisted them in boosting PCE to 19.3%.[28] And Bass et al. demonstrated how humidity could facilitate crystallization.[29] Kamat and co-workers explored the stability of perovskite solar cells stored at 0- 90% RH, to characterize how the PV performance is affected by humidity.[27] The interaction between $CH_3NH_3PbI_3$ and H_2O vapor is investigated by characterizing the ground state and excited state optical absorption properties and probing morphology and crystal structure. **Figure 3** shows top-down scanning electron micrographs of films stored in 0%, 50%, and 90% RH for 14 d. Before water exposure, all of the perovskite films display a somewhat rough surface as seen in Figure 3A–C. After being aged in 90% RH for 14 d (Figure 3F), the perovskite went through a recrystallization process, becoming smooth and highly ordered. Films stored under 0% and 50% RH also show a similar trend, though less severe, structural changes over this period (Figure 3D,E). Same as reported for $CH_3NH_3IPbI_{3-x}Cl_x$ films stored under Ar.[133] Yang and co-workers revealed that a mild moisture environment has a positive effect on perovskite film formation, and the devices showed an average PCE of 17.1%.[134]

Grätzel's group found that PSC fabrication could be carried out under controlled atmospheric conditions and humidity of <1%.[5a] Niu and his team observed that perovskite is sensitive to moisture, and the degradation process was monitored with UV–vis spectroscopy and XRD.[107a] As for as the stability of the device is a concern, Snaith's group showed the enhanced stability of $(HC(NH_2)_2)_{0.83}Cs_{0.17}Pb(I_{0.6}Br_{0.4})_3$ perovskite over 3420 h under continuous 1 sun illumination in the air with an efficiency as high as 18.3%.[136] Chen and co-workers observed that with optimized casting temperature (70 °C) and precursor concentration (1.2 M), the best PCE of 19.54% with J_{sc} of 22.70 mA cm^{-2}, V_{oc} of 1.11 V and FF of 0.78 are achieved with the planar PVSC of ITO/NiO_x/$MAPbI_3$/ PCBM/BCP/Ag. The device performance exhibits excellent thickness insensibility and maintains the PCE over 19% in the wide range of the active layer thickness from 700 to 1150 nm. The unsealed device also shows good stability and remained 80% of its initial efficiency after 30 d storage in the air with an RH of 50%.[137] **Table 1** portrays the PSCs performance under moisture exposure.

3.2. UV Instability

Unlike stability issues associated with moisture, another important factor influencing the stability of perovskite solar cells is UV light exposure. As with multiple solar cell technologies, illumination becomes the reason for degradation in perovskite solar cell.[138] When perovskite films are subjected to both light and dry air the perovskite layer rapidly decompose into methylamine, PbI_2, and I_2 as reaction products.[139] The photogenerated electrons on the perovskite reacted with molecular oxygen to form superoxide, which further reacts with MA of the perovskite absorber. It suggested that replacing the methylammonium component $CH_3NH_3PbI_3$ with species without acid protons could improve tolerance to oxygen and enhance stability.[140] Leijtens et al. reported that a perovskite solar cell with the TiO_2 layer is susceptible to UV induced degradation. This was investigated by measuring 5 h efficiency decay curve, measured under 1 sun AM 1.5G illumination for devices with and without encapsulation and a UV filter. The results showed that encapsulated devices decayed more rapidly than non-encapsulated device, which indicated that the degradation not just start from the active layer but also the meso-TiO_2.[132] The

Table 1. PSCs performance under moisture exposure.

Device configuration	Test conditions	Stability	Refs.
FTO/c-TiO_2/meso-TiO_2/$MAPbI_{3-x}Br_x$/spiro-OMeTAD/Ag	R.H. ≈ 40%	14 d, 93% PCE remained	[307]
FTO/c-TiO_2/meso-TiO_2/$MAPbI_3$/spiro-OMeTAD/Au	R.H. ≈ 24 ± 2%	7 d, 16% PCE remained	[308]
ITO/PEDOT:PSS/$MAPbI_3$/$PC_{61}BM$/Al	R.H. 30–50%	5 d, 0% PCE remained	[75b]
FTO/c-TiO_2/meso-TiO_2/$MAPbI_3$/spiro-OMeTAD/Au	R.H. 60%	18 h, 20% PCE remained	[107a]
ITO/PEDOT:PSS/$MAPbI_{3-x}Cl_x$/$PC_{61}BM$/Ag	Under ambient conditions	275 min, 0% PCE remained	[309]

degradation in the film caused by exposure to light has been explained as[115]

$$2I^- \leftrightarrow I_2 + 2e^- \quad (5)$$

$$3CH_3NH_3^+ \leftrightarrow 3CH_3NH_2 + 3H^+ \quad (6)$$

$$I^- + I_2 + 3H^+ + 2e^- \leftrightarrow 3HI \quad (7)$$

First, the TiO_2 extracts the electron from I^- and then breaks the perovskite structure amounting to the production of I_2. As the acid dissociation constant (pK_a) for the hydrolysis reaction of the methylammonium ion is 10.8, implying that the equilibrium should shift to the left, the incessant elimination of hydrogen ion in reaction and evaporation of CH_3NH_2 drives the reaction[54] forward. Finally, the extracted electrons between TiO_2 and methylammonium lead iodide could return to minimize I_2, and the HI produced evaporates quickly because of its low boiling point.[54,141]

There are various strategies to retard the UV-induced instability of the PVSK devices have been reported. Several groups have demonstrated around 1000 h stability under illumination with slightly or no drops in performance. Saliba and co-workers demonstrated MA-free PVSK solar cells with 1000 h illumination stability via composition engineering.[142] Arora et al. utilized inorganic material CuSCN as HTL. After aging at 60 °C under 1 sun illumination for 1000 h, the corresponding device still preserved its 95% of PCE.[143] Brabec and co-workers used a facile planar structure architecture device employed Ta-doped WOx as HTL prohibited light induced ion-migration, the perovskite solar cells achieve over 1000 h of light stability.[66b] Good stability over 500 h under continuous illumination (AM 1.5) at room temperature was also achieved via contact passivation by using the chlorine-capped TiO_2, the PCE of device maintain its 90% of the original value.[66b]

3.3. Thermal Instability

Thermal stability of PSCs also raises a serious concern, that subjects to a high temperature causing degradation of the device.[144] Some researchers say that the instability of perovskite is linked to the grain boundaries (GBs) or surface,[145] to cap these GBs with suitable protective materials is the attractive strategy to improve the stability of perovskites.[57c,146] It is a well-known fact that temperature has a great effect on crystal structure and phase of perovskite. Previously reported that phase change from tetragonal to cubic occurs at 54–56 °C.[13,147] Solar modules will be exposed to elevated temperature during operation as per international standard (IEC 61 656 climatic chamber tests). The solar cell must require thermal stability up to 85 °C that is corresponding to 0.093 eV.[148] Coings et al. found that perovskite could be decomposed into PbI_2 while heated in nitrogen at 85 °C for 24 hours. They reported the soft matter nature of perovskite layer by investigating morphological, electrical, chemical, and optical characteristics of this new class of material. This experiment was performed in pure dry N_2, pure dry O_2 and at ambient atmosphere with 50% relative humidity for 24 h in the dark.[149] The formation energy of $MAPbI_3$ is 0.11–0.14 eV, which is very close to 0.093 eV suggesting the possible degradation of $MAPbI_3$ at continuous exposure to 85 °C.[109] Philippe et al. investigated thermal stability, the measurements were performed at room temperature, 100 °C, and 200 °C for 20 min. They observed $MAPbI_3$ started to decompose into PbI_2 with an increase in temperature from room temperature to 100 °C and then to 200 °C (given equation show the reaction). The estimated I/Pb and N/Pb ratios gained from hard X-ray photoelectron spectroscopy (HAXPES) results, revealed that $MAPbI_3$ to PbI_2 ratio modified from 85:15 to 70:30 and to 0:100, respectively.[148] The decomposition temperature of perovskite $CH_3NH_3PBI_2$ has been reported as being between 100 and 140 °C.[114,149]

$$CH_3NH_3PbI_3 \rightarrow PbI_2 + CH_3NH_2 + HI \quad (8)$$

To avoid decomposition due to high temperature, the use of thermally resistant materials is the most suitable option.[58] Researchers are trying to achieve a highly efficient and stable perovskite solar cells. Many attempts have been made to improve the stability of perovskite solar cell. Thus far, scientists have succeeded to achieve the stability of more than one year in perovskite solar cells.[125d] Methylammonium lead tribromide ($CH_3NH_3PbBr_3$ or $MAPbBr_3$) is a light absorber compound with a PCE of 7.11%. It also has attracted geometrical stability, maintaining 93% of its initial PCE even after aging of 1000 h.[150] The $CH_3NH_3PbInBr_{3-n}$ perovskite has reported achieving a PCE of 8.54%, with improved stability compared to $CH_3NH_3PbI_3$.[151] Replacement of MA organic cation with a smaller size (MA: 2.17 Å) by HC $(NH_2)_{2+}$ (FA: 2.53 Å) can push the tolerance factor of 0.99, which could potentially enhance the thermal stability.[152] A substantial effort has been now focused on formamidinium lead iodide ($FAPbI_3$) perovskite, which exhibits an ideal bandgap (≈1.48 eV) and significantly enhanced thermal stability.[153] Jin and co-workers reported that $FAPbI_3$ is more thermally stable as compared to $MAPbI_3$ or any other perovskite.[154] Park's team reported good thermal stability in $FAPbI_3$ perovskite at an annealing temperature of 25 °C for 15 min.[155] Although 2D perovskites have demonstrated over

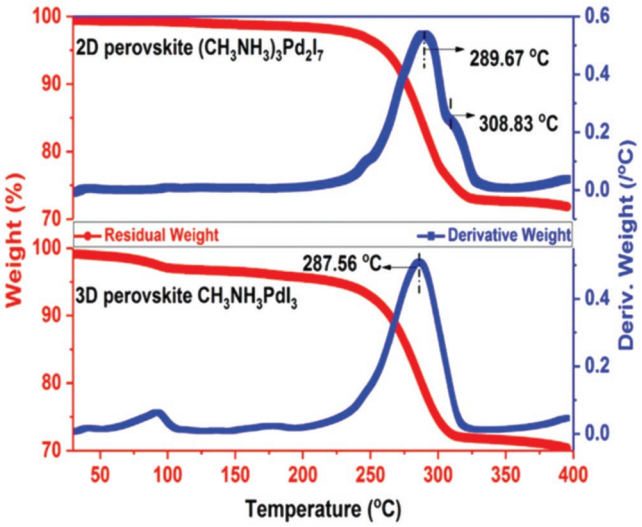

Figure 4. TGA curves of the 3D perovskite and the 2D perovskite. Reproduced with permission.[157] Copyright 2018, American Chemical Society.

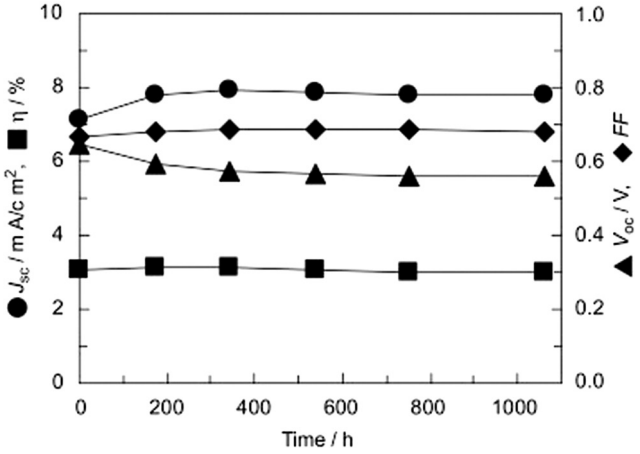

Figure 5. Example of stability tests for the best encapsulated DSCs during a thermal stress test (1000 h @ 85 °C, 85% RH). Reproduced with permission.[161] Copyright 2009, Elsevier B.V.

1000 h device stability.[125d,156] In a quasi 2D perovskite by controlling the orientation, they produced a thin film of near single-crystalline quality, photovoltaic efficiency 12.52% with no hysteresis, improved stability when subjected to light, humidity, and heat stress test. With device encapsulation, the layered devices show a constant value under AM1.5G illumination or humidity for more than 2000 h.[122]

Thermal stability was also explored by thermogravimetric analysis (TGA) measurement.[157] The TGA curves in **Figure 4** revealed that both the 3D perovskite $CH_3NH_3PdI_3$ and 2D perovskite $(CH_3NH_3)3Pd_2I_7$ were thermally stable up to 250 °C, comparable to other hybrid perovskites.[145a,158] Smith et al. reported that a layered 2D perovskite-based on PEA and MA with $n = 3$ exhibited better stability than the archetypical $MAPbI_3$, with a much lower photovoltaic efficiency (4.7%).[57a] This was due to the low carrier mobility on the vertical direction caused by these insulating large organic cation layer supposedly parallel to the electrodes.[159] Dai and co-workers fabricated three MD perovskites by nontoxic transition metal cations (Zn_2^+, Mn_2^+, and Ni_2^+) at 3% to partially replace lead cations in $MAPbI_3$.[160] The MD devices could, respectively, retain 81%, 80%, and 74% of their original PCE values under about 50% RH for 800 h. The PCE of MD perovskite devices maintained 84%, 85%, and 76% of their starting values at 60 °C for 100 h.[160] Leyden et al. demonstrated that solar cells fabricated with $FAPbI_3$ as active layer had better thermal stability than those of $MAPbI_3$. Modules consisted in six series connected subcells with mesoscopic structure (FTO/compact-TiO_2/TiO_2-scaffold/$FAPbI_3$/spiro/Au). FAI (or MAI which was used to fabricate the reference modules) was deposited on PbI_2 films through CVD technique, which permits to control the deposition area by masking.[8] The PCE of modules was lower with regards to small cells (from 10.4% to 9.5%, for the best devices) as a result of issues in the patterning of the spray pyrolysis TiO_2 compact layer and growth of the perovskite over large areas. Recently, Lin and co-workers reported that CSCNT:PEI-based device obtained outstanding stability, sustaining over 94% of original efficiencies after 500 h storage in ambient air and 90% of that after 500 h thermal treatment at 60 °C. The devices also showed good stability exposed to moisture under thermal stress (60 °C, 60% RH), remaining over 70% of original PCEs after 500 h, which could be further raised to 85% while encapsulating the devices with PMMA layer.[105]

Kitamura and co-workers studied thermal stresses using an ionic liquid-based electrolyte and a Pt-coated Ti foil as counter electrode. The performance was not affected by the upscaling processes as demonstrated by comparing cells of both (50×50) mm^2 and (55×300) mm^2 and submodule composed by series interconnecting two or five (55×300) mm^2 cells. Accelerated endurance tests were carried out according to JIS-C8938 on the smallest cell. The best cells demonstrated excellent overall stability both in the 1000 h test at (85 °C,85% RH) conditions as shown in **Figure 5** and in the 200 cycles thermal stress test (heat-cool cycles, between –40 and 90 °C).[161]

The PSCs with modified perovskite structure $((ZnPc)_{0.5}MA_{n-1}Pb_nI_{3n+1})$ offered improved heating stability (**Figure 6**b), device lost only 10% of its original efficiency beyond 1000 h (Figure 6c). The control device with only perovskite film lost over 90% of its original efficiency within 250 h. The color variety of corresponding perovskite films was also prepared to further demonstrate the presence of excellent thermal and moisture stability (Figure 6d).[130]

The outdoor environment would be unpredictable,[162] if someone estimates the lifetime of the device from the indoor test.[163] Hole-conductor-free PSCs based on a triple-layer architecture employing carbon as a back contact was subjected to hot weather in Saudi Arabia desert for one week. No degradation was observed during these outdoor tests. Together with heat exposure during 3 months at 80–85 °C these tests were encouraging.[164]

The mixture of organic cations (methylammonium (MA) and formamidinium (FA)) and mixed halides was used to get a more stable and efficient device.[58] Unfortunately, MA/FA compositions were sensitive to the processing conditions because of their intrinsic structural and thermal instability. Purely inorganic cesium leads trihalide perovskites to exhibit excellent thermal stability.[165] Adding small amounts of inorganic cesium (Cs) in a "triple cation" (Cs/MA/FA) configuration resulted in

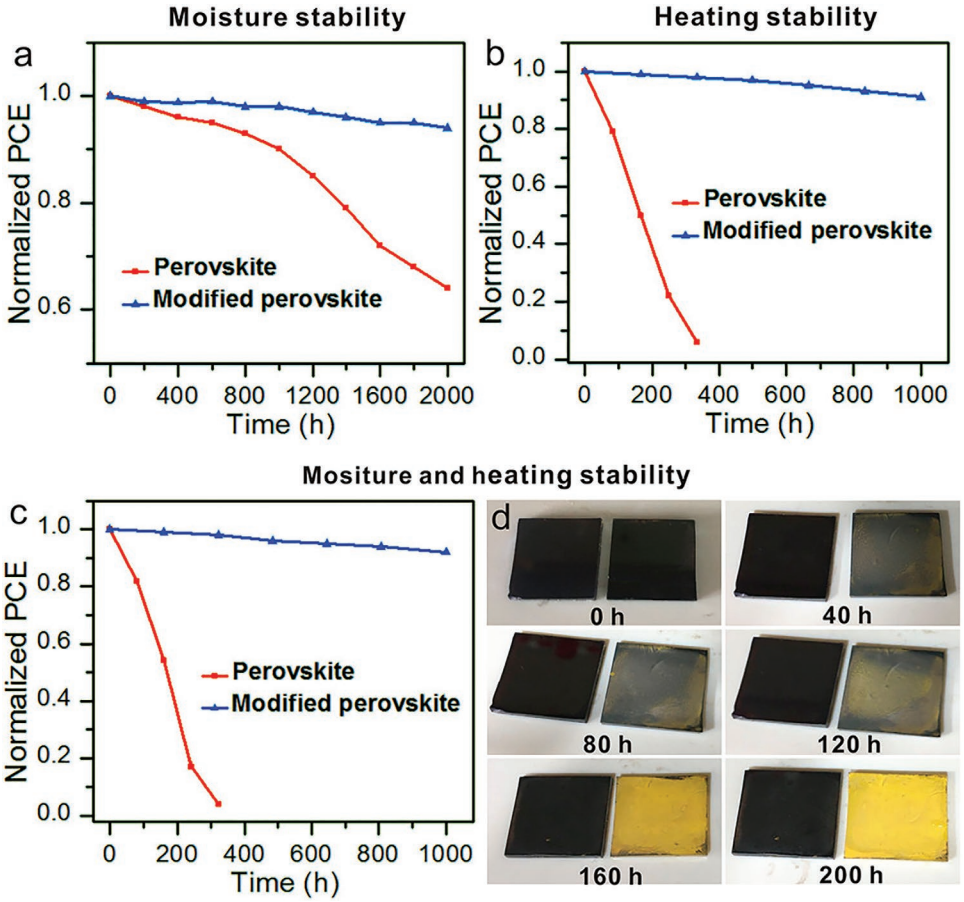

Figure 6. a) Moisture stability measured with a humidity of 45%. b) Heating stability measured at 85 °C in the N_2 environment. c) Moisture and heating stability tested at 85 °C with a humidity of 45%. d) The photos of perovskite films with (left) and without (right) modification stored at 85 °C with a humidity of 45% with different time. Reproduced with permission.[130] Copyright 2018, American Chemical Society.

highly monolithic grains of more pure perovskite.[58] Harvesting this strategy, efficiencies up to 21.1% (stabilized) and an output of 18%, even after 250 h of aging under operational conditions were achieved.[58] Choi et al. present Cs/MA mixtures which prove, in principle, that embedding small amounts of Cs in a $MAPbI_3$ structure could result in a stable perovskite film reaching 8% in PCE.[166] Park and co-workers reported on Cs/FA mixtures showing enhanced thermal and humidity stability, reaching a PCE of 16.5%.[57b] Yi et al. Explained the improved structural stability.[116a]

3.4. Structural Stability

Among the various factors that can affect the stability of perovskite materials, the crystal structure is also an important parameter. There have been several reports that perovskite compounds with organic molecule were unstable in the presence of moisture, oxygen, light, and heat.[40b,167] Therefore, the improvement in the stability of the crystal structure was a critical issue. Various tools and indicators could facilitate the evaluation of crystal structures. Such as, the concept of tolerance factor was proposed to describe the structural stability of the perovskite materials. Goldschmidt tolerance factor (t) is a reliable empirical index to predict which structure is in preference to be formed.[168] Tolerance factor was defined as $t = (R_A + R_X)/\sqrt{2}\,(R_B + R_X)$ where r_A is the radius of the A cation, r_B is the radius of the B cation, and r_X is the radius of the anion. If the value of t is in a certain range, then the crystal present perovskite structure. The value of t should be between 0.8 and 1 for perovskite structure.[169] Nonperovskite structures are formed when the tolerance factor is higher than >1 or lower than <0.71.[168] Advance solar cell technologies toward their maximum efficiency require fragile control over the structural parameters. The rule was developed for oxide perovskite, but the trend is still valid for organic-inorganic hybrid halide perovskite materials.[170] The correlation between the perovskite structure and the tolerance factor is illustrated schematically in **Figure 7**. The organic–inorganic hybrid halide perovskite materials tend to form a hexagonal structure when $t > 1$, orthorhombic structure when $t < 0.8$, cubic structure when $0.8 < t < 1$.[170b]

Recent experimental and theoretical studies showed that the perovskite $(FA\text{-}Cs)PbI_3$ alloying absorbers with effective tolerance factors ≈0.94–0.98 have the best device performance.[116c] The most investigated lead halide perovskite is $MAPbI_3$, which offers tolerance factor 0.91. Poglitsch and Weber investigated the relationship between temperature and the structure of methylammonium trihalide $MAPbX_3$ (X = Cl, Br, I). At room

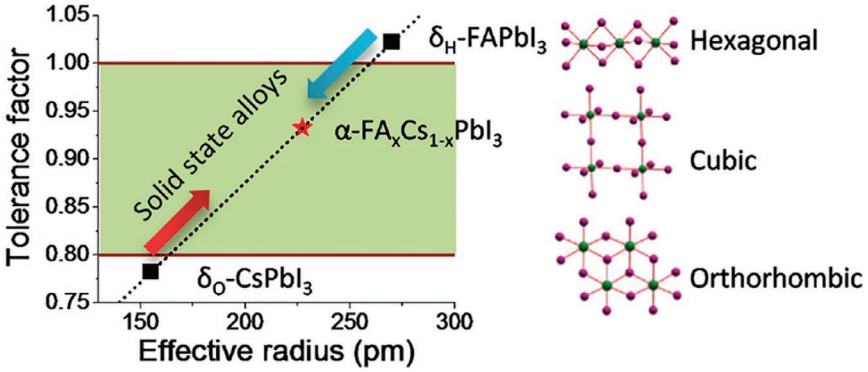

Figure 7. Correlations between tolerance factor and crystal structure of perovskite materials. Reproduced with permission.[116c] Copyright 2015, American Chemical Society.

temperature, both $MAPbBr_3$ and $MAPbCl_3$ present a cubic structure. However, $MAPbI_3$ becomes a tetragonal structure when the temperature increases to 327.4 K.[171] Replacing MA cation (MA: 2.17 Å) by $HC(NH_2)_2^+$ (FA: 2.53 Å) can increase the tolerance factor of 0.99, which could enhance the thermal stability. $FAPbI_3$ does not discolor even at 150 °C under ambient conditions, while $MAPbI_3$ discolors in 30 min.[152,172] One of the most interesting things is that the $FAPbI_3$ could be apt to show the yellow phase (δ-phase),[173] and the tolerance factor is larger than 1, which showed instability, to overcome this problem smaller cations should be incorporated like Cs or Rb could be incorporated into the alloy with FA.[57b,58,174] The doping could lead to the enhancement of thermal stability. The improved stability has been deemed as the enhanced crystallinity of the perovskite layer, the role of tuning the tolerance has not been realized.[11a,175]

A more stable new kind of perovskite, $(PEA)_2$ $(MA)_2$ Pb_3I_{10} ($PEA = C_6H_5(CH_2)_2NH_3^+$, $MA = CH_3NH_3^+$ has also been reported.[57a] Sargent and co-workers adopted $(PEA)_2(MA)_{n-1}PbnI_{3n+1}$ structure, which keeps its almost 3D structure also shows significantly improved stability.[176] According to Goldschmidt's rule, it is reasonable to assume that the tolerance factor was larger than 1 for hexagonal δ-$FAPbI_3$. Yamamoto et al. proposed that the stability strongly depended on the identity of the A-site cation. Cs(B, B′)I_3 structures are stabilized by a mixture of divalent cations, such as Pb, Sn, and Ge, at the B site. Concerning the stabilization mechanisms, Coulomb energy gain seems to be the origin of the structural stability in A = Cs structures. MA(B, B′)I_3 are stabilized by the combination of divalent and trivalent cations, such as the In-Sn and In-Bi systems.[177] The small-size Cs^+ cation results in a tolerance factor too low to sustain a cubic perovskite structure. The photoactive α-$CsPbI_3$ with a bandgap of 1.77 eV is usually attained at a temperature higher than 300 °C.[178] Zhu and co-workers proposed a general chemical composition design protocol to stabilize the perovskite structure, by balancing a material having a large tolerance factor with a material having a small tolerance factor, through solid-state alloying. They reported that the tolerance factor could be tuned by alloying the large-tolerance-factor $FAPbI_3$ and small-tolerance factor $CsPbI_3$ so that α-phase was stabilized in the mixed perovskite. High humidity can trigger the α-to-δH phase transition in $FAPbI_3$ films, but not in the Cs-doped $FA_{0.85}Cs_{0.15}PbI_3$ films, showing the importance of phase stability in $FAPbI_3$-based materials. Due to the stabilized structure, $FA_{0.85}Cs_{0.15}PbI_3$ alloy solar cells showed better performance and device stability against their $FAPbI_3$ counterparts.[116c] Fluorine (F) was introduced into the X-site of ABX_3 to modulate bulk-phase heterostructures and tolerance factors of inorganic $CsPbBrI_{2-x}F_x$ with significantly enhanced PCE and stability.[179]

Given the Goldschmidt tolerance factor, partial substitution of iodine by fluorine in the ABX_3 structure enlarges the low index to stabilize the a-$CsPbBrI_2$ structure. The $CsPbBrI_{1.78}F_{0.22}$ offered superior PCE of up to 10.26% and structural stability. It was also evidenced that $CsPbBrI_{1.5}F_5$ PSCs withstanding constant temperature and humidity retained 69.81% of the initial PCE after 10 d. For lead-free iodide perovskites, $MASnI_3$, $CsSnI_3$, $MASrI_3$, $MABiSI_2$, $MABi_{0.5}Tl_{0.5}I_3$, and $MACaI_3$ have been suggested to be promising candidates by first-principles calculation.[180] Theoretical results indicated that both $MACaI_3$ and $MASrI_3$ form stable phases with similar formation energies and cell parameters compared to $MAPbI_3$.[180c] Wang et al. investigated the structural reconstruction by the first principle.[181] They calculated that phase stability diagrams concerning the chemical potentials of component elements showed that KO (001), O (110), and KO_2 (111) surface terminations possessed the largest stability domain, indicating that they were more likely to be formed compared with other surface terminations. McMeekin et al. and Yi et al. mixed both cations and halides, delivering the possibility of long-term stability through first-principle computations. The majority of blending-ion strategies abide by the tolerance factor within the range of 0.81–1.11. However, the structural stability is still affected by the volatile and hygroscopic nature.[116a,179,182] Marshenya et al. reported better structural stability, moderate thermal expansion, and high conductivity for the using of $PrBaCo_{1.9}Al_{0.1}O_6$-δ cobaltite in various high-temperature solid state electrochemical devices.[183] **Table 2** illustrates the stability of perovskite solar cells with different tolerance factor.

3.5. Influence of Ion Migration on Stability

Unlike traditional photoactive materials such as silicon, the organic–inorganic hybrid perovskite materials show significant ionic characteristics, which restricted the long-term stability of the perovskite materials, owing to the relatively low activation energy for ion migration within perovskite layer.[184] It has been observed that the ion diffusion will become severe when the device subjected to thermal stress, external electric bias, or under the illumination.[185] For example, I^- ions will easily migrate through the polycrystalline PVSK grains and even out of the PVSK layer to interfere with the metal electrode, which generates defects which detrimentally function as nonradiative recombination sites at the grain boundaries.[186]

Tremendous strategies have been utilized to mitigate the ion migration to improve the long-term stability of the PSCs. Liao and co-workers incorporated graphitic carbon nitride into active

Table 2. Stability of perovskite solar cell with a different tolerance factor.

Materials	Tolerance factor	PCE	Stability	Refs.
$Cs_x(MA_{0.17}FA_{0.83})_{(1-x)}Pb(I_{0.83}Br_{0.17})_3$	0.911	21.1%	85% for 250 h	[58]
$MAPb(I_{1-x}Br_x)_3$	0.919	12.3%	Stable for 480 h, 55% humidity	[40b]
$MAPb(I_{1-x}Br_x)_{3-y}Cl_y$	0.925	11.1%	80% for 720 h	[310]
$MAPbI_{3-x}(SCN)_x$	0.834	15.1%	>85% for 500 h, 70% humidity	[311]
$FAPbI_3$	0.987	16.0%	Thermally stable at 230 °C, light stable in humid conditions	[116a]

layer to improve the crystallinity perovskite layer and minimize the defect density further suppressed ion migration, an average PCE of 19.14% was achieved.[187] Yang and co-workers utilized phenylethyl ammonium iodide to stabilize the black phase pure $FAPbI_3$, the activation energy of ion migration determined by the temperature-dependent conductivity enhanced within the presence of 2D perovskite in the grain boundary compared with the bare $FAPbI_3$.[188] The suppression of ion diffusion ensured a PCE as high as 21.07% and an operational stability of 500 h.

4. Influence of Charge Transport Layer on Stability

Apart from the instability of photo active layer itself, to evaluate the device stability, other components such as electron and hole transport layers and electrode need to be considered. The roles of transport layers are 1) providing sufficient charge collection efficiency and 2) forming ohmic contact with the electrode.[78c] To understand the effect of the transport layer on the device stability, we start to review the properties of the transport materials.

4.1. Electron Transport Layer

Highly efficient PSCs generally require good electron selective contact between electron-transporting materials (ETM) and perovskite materials to reduce the potential barrier for electron transfer while blocking the hole transport to minimize the carrier recombination at the interface.[189] ETMs, which extract photogenerated electrons from photoactive layers and transport them to the cathode, also play an important role in photovoltaic performance.[190] A suitable ETM for PSCs should fulfill some requirements such as good energy alignment between the perovskite materials and electrode, high electron mobility, easy dissolution in an organic solvent and good stability in air.[191] The use of organic materials as ETMs offers some advantages like compatibility with flexible substrates,[80b] low solution-processing temperature,[96] negligible hysteresis,[192] and easy fabrication.[81] Common ETMs in n–i–p PSCs include TiO_2, SnO_2, and ZnO, as well as some doped oxides.[193] The ETL in p–i–n PSCs is usually composed of fullerene or one of its derivatives (for example, [6,6]-phenyl-C_{61}-butyric acid methyl ester (PCBM) or indene–C_{60} bisadduct (ICBA).[81] The degradation of the ETMs will result in poor carrier collection efficiency and damage of the ohmic contact with electrode then the performance of the PSCs. Hence, to further improve the stability of the PSCs, it is necessary to understand the deterioration of the ETMs.

4.1.1. Titanium Oxide

Titanium dioxide (TiO_2) has traditionally been used as the ETL for $MAPbI_3$ PSCs, as PSCs historically evolved from dye-sensitized solar cells (DSSC).[132] A compact TiO_2 layer can be fabricated by either spray pyrolysis or a sol–gel method on glass substrates. Vacuum-based processes, such as radiofrequency sputtering,[194] electron-beam evaporation,[195] and thermal oxidation of a sputtered titanium film[196] are also used to generate uniform and high-quality compact TiO_2 films over large areas, but these processes usually require high-temperature annealing. Compact TiO_2 layers have also been deposited by low-temperature techniques, including atomic layer deposition[48,197] and electrodeposition.[163b] Seo et al. used mesoporous TiO_2-based architecture employing the TiO_2 nanoparticles of 200 m^2 g^{-1} surface area, which is much larger than what has been used till now in the conventional mesoporous based devices (60 m^2 g^{-1}). The large area facilitates better contact with the perovskite giving efficient extraction.[198] Mesoporous TiO_2 is commonly applied as scaffold and ETM for high-performance perovskite solar cells due to its appropriate energy level and competent electron collection. Qiu et al. synthesized TiO_2 nanowire arrays as ETM and a considerable perovskite solar cell with a PCE of 4.87% were achieved.[199] Kim et al. proposed the employment of TiO_2 nanorod in perovskite solar cell and found that uniformly ordered and short TiO_2 Nano rod-based layer was desirable as ETM to realize high-performance perovskite solar cell with a PCE of 10%.[193a]

4.1.2. Zinc Oxide

ZnO is an n-type oxide semiconductor that has been used as ETL because of its low crystallization temperature and much higher electron mobility compared to TiO_2. So that is why, ZnO is one of the well-studied alternatives to TiO_2 for its intrinsic high electron mobility,[200] varied morphologies,[201] and its potential in being applied to flexible perovskite solar cells with high bending durability. Numerous processing methods such as sol–gel, hydrothermal, nanoparticle, RF sputtering, ALD, and chemical bath method have been used for the ZnO deposition.[202] The initial examples of ZnO-based PSCs showed poor PCEs of 5.0% or 8.9%,[203] due to a much higher recombination rate caused by the interfacial defects of ZnO layer. Similar to TiO_2, a doping method is also effective to reduce the defects and improve the electron-transporting property for ZnO. Hysteresis-free and stabilized devices with a PCE of 16.1% were achieved using an electron-rich, nitrogen-doped ZnO (N: ZnO) nanorod-based film.[204] Liu and Kelly proposed a solution-processed method and prepared an ultrathin ZnO

nanoparticle layer, which was fabricated as ETL in perovskite solar cell without high-temperature sintering.[205] Nanostructured ZnO layer as ETM in perovskite solar cell was prepared by electrochemical deposition method, that introduced a low n-type doped ZnO as shell to cover as-prepared ZnO nanowires and nanorods layer,by high overvoltage electrochemical deposition, which enhanced the V_{oc} and J_{sc} of subsequent solar cell owing to the suppressed charge recombination, resulting in a considerable PCE of 10%.[206] Compared with the cell based on ZnO, a cell using Al-doped ZnO (AZO) as the ETL exhibited a high PCE of 17.6% and better stability.[207]

4.1.3. Tin Oxide

SnO_2 ETL has been popular in the recent studies because it has a deeper conduction band than TiO_2, resulting in better energy level matching for mixed perovskite compositions (such as $(FAPbI_3)_{0.85}(MAPbI_3)_{0.15}$).[70b] SnO_2 has been considered as a promising ETL candidate since it has excellent electrical properties, even when it is fabricated at a low temperature (<200 °C).[208] SnO_2 films can be fabricated via low-temperature processing routes using the as-prepared nanoparticles,[74a] sol-gel-derived tin precursors,[193b] or atomic layer deposition technique.[70b] Song et al. formed a planar perovskite solar cell by replacing TiO_2 with SnO_2 as the electron selective contact.[209] Kuang et al. introduced a PCBM interfacial layer between the SnO_2 and the perovskite significantly reduced the hysteresis. The SnO_2 deposited at 200 °C exhibted a more stable cell performance more than 16 h under continuous AM 1.5G illumination.[210] Huang and co-workers reported improved device efficiency from 14.05% to 16.87% with enhanced stability by introducing dopamine (DA) self-assembled monolayer (SAM) on the top of the SnO_2 ETL to modify the SnO_2/perovskite interface.[211] The most used contact layers of perovskite such as TiO_2 or ZnO degrade significantly to 10–30% of the initial value after only dozens of hours storage.[212] As for as SnO_2 is concern, the relatively wide bandgap SnO_2 enables it to absorb less UV light with better device stability. Moreover, the lower hygroscopicity and acidity resistance of the SnO_2 also contribute to the durability of the PSC device.[209] Zhu et al. utilized the hydrothermal method to prepare highly crystalline SnO_2 nanocrystals with good electron-transporting properties, and the relatively thick film of SnO_2 (≈20 nm) gave a promising PCE of 18.8% for PSCs with over 90% of the initial PCE retained after 30 d storage in an ambient with about 70% relative humidity.[213]

4.1.4. Fullerene and its Derivatives

Fullerene has many fascinating features, such as high electron mobility,[214] high electron affinity,[215] etc. Because of their well-matched energy level with perovskite, fullerene-based materials have been widely employed as in PSCs as an electron transport layer. Outstanding merits that make fullerene-based interlayers imperative defect passivation, efficient charge extraction, and alleviation of hysteresis instabilities in encompassing PSCs.[216] Fullerenes can effectively passivate the trap states at the surfaces and grain boundaries of the perovskite layer, relating to the formation of fullerene–halide radicals that suppress the formation of deep trap states. C_{60} is the most widely used fullerene as ETM in PSCs. The perfectly symmetrical structure of C_{60} guarantees well $\pi-\pi$ tacking, making C_{60} have a comparatively higher electron mobility than that of the anisotropic C_{70} with a value of 1.3×10^{-3} cm^2 $(V\ s)^{-1}$.[217] C_{60} can be packed more densely than PCBM to facilitate intermolecular charge transport and shows much higher electron mobility and conductivity compared to PCBM. Chen and co-workers have pioneered the use of fullerene C_{60} and its derivatives [6,6]-phenyl C_{61}-butyric acid methyl ester ($PC_{61}BM$) or indene-C_{60} bisadduct ($IC_{60}BA$) as the electron transport layer in p–i–n PSCs. Although the PCE was 3.9%, their work demonstrated the feasibility of fullerene materials as the ETL for p–i–n PSCs.[81] Huang and co-workers employed unique double fullerene layers as the electron extraction layer, boosting the fill factor (FF) to above 80% and PCE to 12.2%.[95] Yoon et al. reported hysteresis-free planar PSCs based on $MAPbI_3$ with a PCE of 19.1% and good device stability against mechanical bending. PCE decreased by ~20% after 1000 cycles using a room-temperature vacuum-processed C_{60} ETL.[218] A new fullerene derivative C_5-NCMA was designed to replace the commonly used $PC_{61}BM$ as ETLs in p–i–n PSCs,[219] which significantly enhanced the device stability to moisture. A dimeric fullerene derivative D-C_{60} was also applied as ETL in PSCs.[220] Devices based on D-C_{60} exhibited PCE of 16.6% and higher stability than $PC_{61}BM$. Jung et al. designed non-fullerene organic ETMs based on NDI cores for high-performance, low temperature, solution-processable PSCs.[221] The devices have greater than 20% PCE and long-term stability by keeping 90% of their initial PCE after 500 h under 100°C without encapsulation.

4.1.5. Others

Tin doped zinc oxide (ZSO) was also used as ETL in inverted planar PSCs. Jen and co-workers used the hydrothermal method to prepare crystalline ZSO NPs and applied them as an ETL via a simple room-temperature solution process. They got PCE of 17.7%, and the device showed good ambient stability, retaining over 90% of its original PCE after being stored under ambient conditions for 14 d under 30 ± 5% relative humidity.[222] $SrTiO_3$ is a typical ternary metal oxide that was developed as an ETM in dye-sensitized solar cells and polymer solar cells.[223] Bi_2S_3, known as a ribboned compound with intrinsic high mobility and stability, could be used as the ETL for PSCs. Li et al. prepared a compact and smooth amorphous Bi_2S_3 ETL, which improved the ambient storage stability without sacrificing the PCE of inverted PSCs.[224] $BaSnO_3$ has been successfully applied in dye-sensitized solar cells and PSCs as ETM. Recently, a crystalline superoxide-molecular cluster colloidal solution was developed to deposit La-doped $BaSnO_3$ below 300 °C. They achieved a PCE of 21.2% and retained 93% of their initial value after 1000 h of full-Sun illumination.[225]

4.2. Hole Transport Layer

HTMs generally obliged to lower the transporting barrier and block the electron transport between perovskite and electrode

with less carrier recombination to boost the device efficiency. HTMs play a critical role in boosting the efficiency of PSCs.[226] In particular, the HTL in conventional structures plays an important role in transporting holes, blocking electrons, and protecting the perovskite from external factors, including moisture, heat, and oxygen.[227] To achieve a highly efficient and low-cost inverted PSCs, much effort has been devoted to the discovery of high-performance HTLs.[228]

4.2.1. PEDOT:PSS

PEDOT:PSS is a cheap polymer with high conductivity. PEDOT:PSS can be applied as an HTM layer in the inverted structure, and it is usually located on the bottom of devices.[59c,229] PEDOT has good conductivity but low solubility. In this case, PSS is combined with PEDOT to increase the solubility. When PEDOT:PSS was dissolved in water, the ionization will happen, and two PSS chains will separate one PEDOT chain. Jeng et al. first demonstrated an inverted PSC using PEDOT:PSS as the HTL and PCBM as the ETL.[81] Sun et al. used PEDOT: PSS and $PC_{61}BM$ as the HTL and ETL, respectively, and studied the $MAPbI_3/PC_{61}BM$ bilayer solar cell interface and demonstrated an improved FF of up to 0.76 with a 7.4% PCE.[78a] Until now, PEDOT:PSS has been the most popular HTL material due to its good processability, high thermal stability, good mechanical flexibility, sufficient optical transparency, and proper energy levels. The thickness ranges from 10 to 20 nm depending on the viscosity of PEDOT:PSS solution and the deposition rate.[230] Hu et al. reported enhancement in V_{oc} and stability in the ambient environment. By water rinsing the spin-coated PEDOT:PSS films, the perovskite solar cells showed an improvement in PCE from 13.4% to 18.0%.[231] However, in p–i–n planar PSCs, poly(3,4-ethylene dioxythiophene) poly(styrene sulfonate) (PEDOT:PSS) was widely used as the HTL due to its high work function (about 5.0 eV), high transparency, and good wettability with a perovskite layer.[232] The performance of PEDOT:PSS-based PSCs was continuously optimized by doping with PEDOT:PSS or introducing an interlayer at the interface of the PEDOT:PSS/electrode or PEDOT:PSS/perovskite.[233] Choi et al., therefore, abandoned PEDOT:PSS altogether and achieved a significant improvement in device stability in the air by employing a pH-neutral polyelectrolyte.[86] The acidic PEDOT:PSS can etch indium tin oxide (ITO) and decompose perovskite, which results in poor stability of the devices.[90] MoO_3 is one of the most promising HTL materials because of its nontoxicity and ambient condition stability. MoO_3:PEDOT:PSS composite film as the HTL in a polymer solar cell to take advantage of both the high conductivity of PEDOT:PSS and the ambient condition stability of MoO_3, and eventually both PCE and stability were improved.[234] Hou et al. reported that MoO_3/PEDOT:PSS bilayer structure as the hole-transporting layer improve the efficiency and stability of planar heterojunction perovskite solar cells, only 7% degradation in PCE was observed under ambient conditions for 10 d.[235]

4.2.2. Spiro-OMeTAD

Commercially available triarylamine-based materials, e.g., spiro-OMeTAD is most commonly used as HTM,[236] because of their suitable energy level, high solubility, amorphous character, and high glass transition temperature.[236] In 2012, solid-state DSSCs based on $CH_3NH_3PbI_3$ demonstrated a PCE of 9.7%, in which spiro-OMeTAD was used as the HTM.[21] Researchers largely focused on the spiro-OMeTAD as the HTM layer due to its prominence and widely usage history. To overcome the instability of spiro-OMeTAD layer, several approaches are reported. In the work of Liu and co-workers, they instilled a tetrathiafulvalene (TTF) derivative into PSC without any p-type dopants.[115] Another suggestion was to solve the instability of the PSC due the spiro-OMeTAD layer is to take it out of the device.[237] The stability of spiro-OMeTAD that mainly originates from its amorphous nature and its relatively high glass transition temperature brought attention to different potential applications in optoelectronics.[236] Bach et al. introduced spiro-MeOTAD in DSSCs and used it as an efficient heterojunction layer formed with dye absorbers providing a high yield of photon-induced electric current.[19] Spiro-MeOTAD was adapted in PSCs leading to a breakthrough in PCE exceeding 22% as well as substantially enhanced stabilities.[238] Kim et al. replaced the liquid electrolyte by the solid spiro-OMeTAD HTM in the perovskite light absorber solar cell.[21] Domanski et al. employed a thin layer of 10 nm of chromium between the spiroMeOTAD HTM and the top gold electrode.[239] The Cr layer enhanced the stability of the PSCs. The alteration to the solid spiro-MeOTAD HTM provided a substantial increase in PCE and stability, exceeding 10% of PCE, and stable operation of 500 h in the air without any encapsulation. Also, a record PCE of 22.1% was achieved.[240] Spiro-OMeOTAD was adapted in PSCs leading to breakthroughs in PCEs exceeding 22% as well as substantially enhanced stabilities.[241] Bui et al. designed and synthesized simple chemical routes,[242] B74 and B186 supposed to operate as efficiently as the benchmark Spiro-OMeTAD compound. These compounds showed high thermal stability, adequate morphology, and improved hydrophobic properties. Bis(trifluoromethane)sulfonimide lithium salt (LiTFSI) and *tert*-butyl pyridine (TBP) are widely doped in spiro-OMeTAD. LiTFSI attracts water, which results in accelerated degradation of perovskite.[243] In addition, the gradual evaporation of TBP and its reaction with the perovskite led to a new threat to the long-term stability of PSCs.[243] Cheng and co-workers reported high PCE of 18.4% in the TBATFSI-included devices.[244] The PSCs based on TBA-TFSI and TBA-PF_6 show significantly enhanced environmental and thermal stability, by maintaining more than 60% of the initial efficiency after 1 month of aging in the dark with 50% humidity and after 8 h of heating at 85 °C in ambient conditions (50% humidity). Mali et al. introduced a new naturally extracted cross-linked carbon nanoparticles as hole transport layer (C-HTL).[245] The aloe vera processed carbon C-HTL based PSCs yields up to 12.50% PCE, with enhanced air and moisture stability >1000 h at 45% relative humidity.

4.2.3. PTAA

As a replacement of Spiro-OMeTAD, poly [bis(4-phenyl) (2,5,6-trimethylphenyl)amine] (PTAA) first employed as the HTL in the normal structure for PVSK solar cells by Seok and co-workers.[54] This use of the polymeric HTL, delivered a PCE

of 12.0% with a enhanced V_{oc} of 0.997 V, J_{sc} of 16.5 mA cm^{-2} and FF of 72.7%. One the other hand, Huang and co-workers first introduced PTAA doped with 2,3,5,6-tetrafluoro-7,7,8,8-tetracyanoquinodimethane (F_4-TCNQ) as the HTL in the inverted structure, a champion PCE of 17.5% was achieved.[246] This hole transporting layer has been proved to be an ideal candidate to tackle the instability of device, especially under the illumination and the elevated the temperature.[247] Snaith et al. realized a champion efficiency of 23.6% under 14 suns illumination and retain its more than 90% PCE after 150 h under 10 suns with PTAA as HTL.[247] Han et al. employed PTAA doped with 4-isopropyl-4′-methyldiphenyliodonium tetrakis (pentafluorophenyl)borate (TPFB) as HTL in CIGS/PVSK tandem solar cells, a certified 22.43% was realized and the devices under ambient conditions preserved 88% of their original values under full sun illumination.

4.2.4. Inorganic Materials

Inorganic HTMs are potentially superior replacements because they exhibit higher mobility and stability in comparison with organic HTMs. Recently, reasonable efficiencies have been reported for planar (18.51%) and mesoporous structured (20.4%) PSCs with $CuGaO_2$ and CuSCN, respectively.[143] Inorganic HTM such as NiO_x have shown some promise to improve cell stability. The NiO_x can be a suitable candidate due to its p-type characteristics with a wide bandgap (E_g > 3.50 eV), high optical transmittance, sufficient conductivity, chemical stability, and an energetically favorable energy level alignment with various photoactive absorbers.[248] The choice of NiO_x–HTM in PSCs has also shown 90% stable performance for over 60 d of storage in air.[75b] Xiong et al. demonstrated one-step hydrothermal-processed NiO nanosheet network, the developed PSCs maintained 75% of its efficiency after 500 h.[249] Tan and co-workers reported that the VO_x-HTL-based p–i–n-type planar PSCs achieve a PCE value of 14.5% with better stability than PEDOT: PSS-HTL-based devices due to the better stability of VO_x.[250] VO_x HTL retains 65.7% of the initial PCE after aging for 500 h in the ambient environment (RH: ≈25%) without encapsulation. Jiu and co-workers developed a facile solution method to prepare a V_2O_5 film combined with P3CT-K that form a bilayer structure as hole-transporting layers in inverted $CH_3NH_3PbI_3$ solar cells.[251] The device based on bilayer HTL exhibited a higher PCE of 19.7%. As for as the stability of the device is concern 86% efficiency was maintained even after one month.

4.2.5. Others

Han et al. reported organic-inorganic hybrid HTL which was composed of the unhoped spiro-OMeTAD and Cu_9S_5 layer.[252] The modified hole and electron transport layers were applied in n–i–p perovskite solar cells. Finally, it achieved a PCE of 17.10% and retained about 96% of PCE after 1200 h in an ambient atmosphere without any encapsulation. Park and co-workers reported improved stability with PCE of 21.44% by WO_3/spiro-OMeTAD hybrid HTLs.[253] **Table 3** highlights the types of THMs and ETMs along their efficiency and stability.

5. Role of Electrode Materials

5.1. Electrode Materials

Although the electrode materials are not in direct contact with the perovskite layer, the stability of electrode materials is also important for long-term operation. The electrode is the uppermost layer, which is closest to the environment.[254] A perovskite solar cell (PSC) is a structure that usually comprises a substrate, electrodes, a perovskite photoactive layer, together with necessary charge transport layers. So the electrode must be robust enough to slow down the moisture penetrating into the perovskite layer. Han and co-workers adopted the thick carbon as the electrode and delivered the efficiency as high as 12.8%, and the devices showed good stability under 1000 h light soaking.[11a] Ag or Au is usually employed as the top electrode in perovskite solar cells. Silver electrodes react with halide to form silver halides.[255] Although gold electrodes are more

Table 3. Types of HTMs and ETMs along their efficiency and stability.

Device structure	Efficiency	Stability	Refs.
ITO/ZnO-JTCA/$MAPbI_3$/spiro-MeOTAD/Au	18.82%	70% left after 840 h in air	[312]
ITO/PEDOT:PSS/$MAPbI_{3-x}Cl_x$/PCBM/ZnO/Al	16.8	Excellent stability	[71]
ITO/5 at%Cu:NiO_x/$MAPb(I_{1-x}Br_x)_3$/$PC_{61}BM$/BCP/Al	15.40	244 h stability	[313]
ITO/NiO (80 nm)/$MAPbI_3$/ZnO (70 nm)/Al	16.1	>60 d stability	[75b]
FTO/SnO_2/$FA_{1-x}(MACs)_xPbI_3$/spiro-MeOTAD/Au	20.7%	83% left after 60 h	[71]
FTO/TiO_2/$MAPbI_{3-x}Cl_x$/sputtered NiO_x/Ni	7.28	>2 months stability	[314]
FTO/NiO_x/$FA_{1-x}MA_xPbI_3$/PCBM/TiO_X/Ag	20.65%	90% left after 500 h under 85 °C	[315]
ITO/PTAA/$(FA_{0.83}MA_{0.17})_{0.95}Cs_{0.05}$ $Pb(I_{0.6}Br_{0.4})_3$/ICBA/C_{60}/BCP/Cu	18.3%	90% left after 720 h in N	[316]
FTO/BI-TiO_2/Mp-TiO_2/FA-perovskite/spiro-OMeTAD/Au	20%	800 h	[317]
FTO/bl-TiO_2/mp-TiO_2/RuCsFAMA$PbI_{1-x}Br_x$/spiro-MeOTAD/Au	21.8%	95% left after 500 h under 85 °C	[318]
FTO/bl-TiO_2/mp-TiO_2/CsFAMA$PbI_{3-x}Br_x$/CuSCN/RGO/Au	20.4%	95% left after 1000 h under 60 °C	[143]
FTO/TiO_2/Al_2O_3/PVK/P3HT/SWNT/PMMA/Ag	15.3%	80% for 96 h, 80 °C	[1a]

stable, gold can diffuse in the perovskites and cause irreversible device degradation.[239] To develop high-performance and foldable flexible thin-film photovoltaics, several transparent electrodes, such as polymer electrodes, metal oxide/metal/metal oxide stack electrodes, carbon nanotubes/graphene, and metal electrodes have been used as substitutes for the flexible ITO/FTO electrode.[256]

5.2. Electrode Degradation

The high sensitivity of the perovskite layer to water, oxygen, and temperature is the initial reasons for its poor stability. Beside the perovskite layer, the degradation of the interface layer and electrode was also the reason for the causes of degradation.[257] Ag or Au is usually employed as the top electrode in perovskite solar cells. Among all the factors that cause the instability of perovskite solar cells, the reaction between common electrode materials and the perovskites creates significant degradation. Exposure of devices to the stressful environment might result in decomposition of the top electrode. Kato et al. studied the mechanism of degradation of the Ag electrode using X-ray diffraction (XRD) and high-resolution X-ray photoelectron spectroscopy (HRXPS).[255] It was proposed that the exposure to moisture made pin holes in the spiro-OMeTAD layer and volatile byproducts containing iodine, then volatile component diffused into the Ag layer to form AgI. Note that the formation of metal iodides on the surface of the electrode can also cause solar cell degradation.[255] Even noble metals, such as expensive gold (Au), were found to react with hybrid perovskite in short-term studies.[258] The diffusion of Au across the thick hole transport layer resulted in the degradation of the devices in several hours.[239] The chemical reaction between the perovskite layer and top electrode through the migration of iodine or metal atom was the critical problem that leads to inferior device stability.[259] The corrosion of Ag and Al electrodes by hybrid perovskites has been generally ascribed to the chemical reaction of the metal electrodes with the decomposition products of perovskites.[260] Yang et al. created a solid-state electrochemical cell consisting of Pb, $MAPbI_3$, AgI, Ag to monitor ionic movement.[261] Such a coulometric cell configuration with one electronic (Pb) and one ionic electrode (AgI, Ag) causes chemical changes during current flow.

5.3. Effect of Electrode Materials

Generally, Ag, Al, and Au are among the most commonly used electrodes in $MAPbX_3$ optoelectronic devices. Metal electrodes such as Au, Ag, and Al have stability issues as well. Ag and Al electrodes suffer from corrosion by ion migration in perovskite, resulting in an apparent color change and PCE decay.[259] Recently, Cr electrodes have been used in high-energy radiation detectors based on single-crystalline $MAPbBr_3$.[135] Hu and co-workers investigated the effects of electrode material on the electrical properties in single crystalline $MAPbBr_3$ devices.[262] They reported that Cr contacts greatly reduce the amount of hysteresis at the metal/$MAPbBr_3$ interface; Cr contacts increase the interfacial resistance of the sample by over a factor of 100, which reduces the amount of interfacial recombination. Greater electrode stability could also be achieved by moving away from using either Ag or Al, and instead employing a Cr_2O_3/Cr electrode, which is shown to be chemically inert toward iodide.[258] Inserting a thin Cr layer between the Au electrode and the HTM prevents the Au diffusion into $MAPbI_3$ and leads to a lower but stable PCE.[239] Ku et al. have pioneered a very promising approach to employ a thick carbon electrode.[11b] Carbon material based counter electrodes have been employed in the HTM-free perovskite solar cell.[22] The thick carbon counter electrode seems to be one of the best choices due to its protection from humidity. In some architecture, devices using the carbon cathode do not even require a selective p-type contact.[11b] The application of a carbon electrode has made the device preparation easier via screen printing, which is favorable for achieving large-scale production. PSCs with a porous carbon back electrode usually exhibit exceptional long-term stability (>1000 h) under light and ambient conditions.[11a] In order to fabricate stable perovskite solar cells, diffusion barrier layers were often needed to be inserted to separate the metal electrodes and the perovskite layer.[263] Zhao et al. recently reported that the $MAPbI_3$ solar cell with a Cu electrode in an inverted configuration (ITO/PEDOT/$MAPbI_3$/Cu) has a stable PCE (>20%) without CuI formation at the $MAPbI_3$/Cu interface even after prolonged annealing of the device at 80 °C.[264]

Silver nanowire (AgNW) electrodes have received substantial attention in the last few years, and become the most promising solution processable electrodes for using in perovskite solar cells.[265] Lin and co-workers reported spin-coated AgNW transparent metallic electrode,[266] an overall PCE of 11.1% could be obtained from front illumination, and ≈70% of the original PCE could be maintained when illuminated from the transparent electrode side. Double-layer electrodes, such as Cr_2O_3/Cr, MoO_x/Al and ZnO/Al, have shown improved stability in PSCs.[77b,267] Lai reported nickel/gold/copper (Ni/Au/Cu) trilayer transparent electrode with a PCE of 11.1%.[268]

6. Encapsulation

The performance of PSC devices is known to be highly susceptible to deterioration upon exposure to ambient atmospheric conditions, due to the susceptibility of the perovskite to decompose when in contact with moisture. The outermost modification to enhance the stability of a perovskite solar cell is the encapsulation of a device. The device encapsulation will play a role in the commercialization of perovskite solar cells. Devices without encapsulation commonly exhibited severe degradation under continuous illumination after several hours,[269] while encapsulated devices exhibited longer lifetime.[270] Encapsulation strategy involves a material, which is resilient against moisture and oxygen permeation,[271] which is used to encapsulate the device with the placement of electrode strip, which can still be accessed without compromising the integrity of the protective encapsulation. Encapsulation is an important component of photovoltaic devices, as this protects it from damaging effects of oxygen and moisture.[272] Typically, the device is covered by a thin glass coverslip, which is sealed using a UV curable epoxy resin.[132]

6.1. Encapsulation Techniques with Improved Stability

Much work on the effectiveness of various encapsulation techniques has been carried out in the field of photovoltaics, as degradation is one of the major factors compromising the stability of solar cells. One of the famous encapsulation technique, borrowed from the organic light emitting diode technology (OLED) consists of a cover glass lid and UV epoxy sealing with the addition of a piece of desiccant. This combination improved the device stability.[273] The interesting thing it was shown that partial encapsulation allowed direct contact to the electrodes and thus penetration of moisture through the edges resulted in shorter lifetimes compared to full encapsulation with protected edges.[274] Obviously, careful encapsulation can significantly extend the device lifetimes. Krebs et al. developed a methodology for fully roll to roll processed polymer solar cells.[275] Encapsulation was performed by attaching a 25 µm thick PET barrier foil with an acrylic adhesive. The simple encapsulation slightly improved device stability. Tanenbaum et al. improved this technique by sealing the edges, resulting in largely improved device stability.[32c] Single- layer thin films are attractive because of the simplicity of the manufacturing process.[276] While multilayer films are widely used for encapsulation of organic photovoltaic devices and often consist of alternating organic and/or inorganic layers.[277] As for as encapsulation architecture is concern Russian Doll architecture is utilized.[278] A two-step encapsulation approach using first low temperature (<100 °C) curing materials followed by a second sealing step at a higher temperature (130 °C) was found to be effective and resulted in better device performance.[279] Hwang et al. showed that they could also improve the performance lifetime of a device by spinning a layer of amorphous teflon on top of the device.[280] Chang et al. used the concept of a dense alumina layer as a protective barrier and showed that the atomic layer deposition of an Al_2O_3 layer significantly improved the air stability.[281] Anta and co-workers investigated a simple solvent-free polymer encapsulation method for perovskite solar cells using a conformal plasma polymer thin film,[282] and improved device stability has been demonstrated not only under moisture exposure and illumination but also when the devices were exposed to humid air and even immersed under water. Weerasinghe et al. and his team used two encapsulation architectures partial and complete encapsulation,[283] and they observed partially encapsulated devices retained more than 80% of their initial PCE for over 400 h with a rapid performance loss observed after 400 h. The devices encapsulated using the complete encapsulation architecture was stable throughout 500 h. Organic/inorganic multilayer TFE system showed outstanding barrier property fabricated by initiated CVD coupled with the ALD process.[284] Im and co-workers reported PSC maintained 97% of its initial value after exposure to 50 °C and 50% RH for 300 h surrounding conditions, confirming the enhanced stability of the PSC against moisture by thin film encapsulation.[285]

6.2. Encapsulation Materials

A variety of materials have been investigated as device encapsulants including teflon, Al_2O_3, poly (methyl methacrylate) (PMMA) and polycarbonate (PC) etc. SiN_x thin films can be deposited using radio frequency (RF) plasma enhanced chemical vapor deposition (PECVD) and low frequency (LF) PECVD.[286] Alternating SiO_x and organosilicon layers deposited by PECVD on a poly(ethylene naphthalate) (PEN) substrate are introduced for encapsulation.[287] In the case of encapsulated devices based on Poly[2-methoxy-5-(3, 7-dimethyloctyloxy)-1,4-phenylenevinylene] (MDMO-PPV), V_{oc} remains at about 90% of its initial value after 3000 h. SiO_x/SiN_x/parylene based inorganic encapsulation films showed limited barrier performance due to microdefects.[288] Encapsulation by Al_2O_3 deposited using ALD is further demonstrated by the performance of pentacene/C_{60}-based OPV cells. These cells are found to be stable for 6000 h in ambient conditions with negligible deterioration in properties.[289] Al_2O_3/SiO_2 bilayers (26 and 60 nm, respectively) can reduce the effective water vapor transmission rate (WVTR) to 1×10^{-4} g m^{-2} d^{-1}, as opposed to $\approx 1 \times 10^{-3}$ g m^{-2} d^{-1} for the 26 nm thick Al_2O_3 layer.[290] By the concept of Al_2O_3/SiO_2 bilayers, it is possible to reduce this corrosion substantially and improve the gas diffusion barrier performance. Ethylene vinyl acetate (EVA) is among the most widely used encapsulating materials of the single-layer encapsulation films available, it offers weather resistance and long-term reliability under long periods of exposure to different elements.[291] Ethylene-methyl acrylate (EMA), the key benefits of EMA are its thermal stability, adherence to various substrates, chemical resistance, and good mechanical behavior at low temperature. Therefore, it is used for encapsulation purpose.[292] Polyvinyl butyral (PVB) can be used as encapsulation layer, which is already widely applied in the modern mass production of thin film solar cells.[293] It can strongly reduce the moisture permeation and ensure longer lifetime.[278] For creating commercially viable encapsulation structures for flexible OPV devices, a commercial polymer cyclized perfluoropolymer was reported.[294] This material is widely used in organic light emitting diodes (OLEDs). OLEDs are even more sensitive to oxygen/water-vapor degradation than OPV. Cyclized perfluoropolymer may provide barrier needed for commercially viable, flexible, printable solar cells. Tantalum–silicon–oxygen (Ta–Si–O) establishes a highly efficient barrier against humidity diffusion.[295] Investigations showed that a 10 nm thick Ta–Si–N layer deposited onto a Ta–Si–O layer reduced CIS solar cell degradation at an accelerated aging test. Watson and co-workers presented a straightforward method for screening different encapsulants by using time-lapse photography on perovskite layers only and the change in RGB values to monitor their degradation.[296] We summarize the encapsulated devices along with their stability in **Table 4**.

7. Economic Feasibility of Perovskite Devices

Before establishing the technology of any new type of solar cells, there are many established capital cost and operating cost issue that need to be dealt with carefully.[297] An economical way of looking at solar cells is by evaluating the energy payback time (EPBT) of different solar cells. EPBT can be calculated by a formula given by Bhandari et al.

Table 4. Encapsulated devices along with their stability.

Device structure	Testing conditions	Initial PCE	Remaining PCE	Refs.
FTO/c-TiO_2/mp-Al_2O_3/$MAPbI_{3-x}Cl_x$/spiro MeOTAD/Au	1000 h at 40 °C	12.3	50%	[132]
FTO/C_{60}/mp-Al_2O_3/$MAPbI_{3-x}Cl_x$/spiro MeOTAD/Au	500 h at 60 °C	10.4	55%	[319]
FTO/PEDOT:PSS/$(BA)_2(MA)_3Pb_4I_{13}$/PCBM/Al	Under 1 sun 2250 h, 65% RH	12.52	100%	[122]
FTO/c-TiO_2/mp-TiO_2/$(FAPbI_3)_x(MAPbBr_3)_{1-x}$/ spiro-MeOTAD/Au	3 months outdoor	18.7	95%	[320]
FTO/LiNiO/$Cs_{0.05}FA_{0.7}MA_{0.25}PbI_3$/$C_{60}$/Al	1 sun	20.5	85%	[321]
$FA_{0.83}Cs_{0.17}Pb(I_{0.6}Br_{0.4})_3$	4000 h in air	17.5 ± 1.3	80%	[125c]
FTO/c-TiO_2/$MAPbI_3$/spiro-MeOTAD/Au	500 h at 45°C	13.9	90%	[322]

$$\mathrm{EPBT}\left(\mathrm{years}\right)=\frac{\text{Embedded primary energy}\left(\mathrm{MJm^{-2}}\right)}{\text{Annual primary energy generated by the system}\left(\mathrm{MJm^{-2}\ year^{-1}}\right)}=\frac{\mathrm{W1}}{\mathrm{I}\times\eta\times\mathrm{PR}/\varepsilon}$$

where W_1 is embedded primary energy, ε is electricity to primary energy conversion factor (usually 0.35); I is the total solar insolation incident on a unit surface per year, η is the average module efficiency, and PR is the system performance ratio.

Another way of looking at the solar cell is to evaluate the energy return on energy invested (EROI),[297] which is a function of EPBT and lifetime, given as

$$\mathrm{EROI}=\frac{\mathrm{lifetime}\left(\mathrm{years}\right)}{\mathrm{EPBT}\left(\mathrm{year}\right)}$$

The EROI is presently put up as a 3:1 ratio for any solar cell technology to be viable. Apart from the architecture of the cell, the energy embedded in the manufacturing of materials another critical consideration in the solar insolation, which affects the EPBT. Most studies take the average of 1700 KWh m^{-2} $year^{-1}$.[298]

Silicon-based PV modules have taken the same role in the power industry as has been the role of silicon complementary metal–oxide–semiconductor (CMOS)-based integrated circuits in microelectronics and nanoelectronics. Falling prices of PV modules[299] are largely responsible for the exponential growth of the PV industry in recent years.[299] The material cost of a lead iodide perovskite absorber layer (≈400 nm thick) is quite low, around US$2 per square meter of the module.[300] So we can say that perovskite is the cheapest component in the structure but the transparent conductive substrates (FTO or indium tin oxide) of low sheet resistance (<10 ohms per square), which cost around US$10 per square meter. The thin-film PV module share is expected to decline from 8% in 2014 to 7% in 2015, compared to 15% market share in 2010.[299] However, lead is toxic, and its environmental impact should be assessed before commercialization of lead PSCs.[301] The restriction of hazardous substances of the European Union strongly regulates the use of Pb in industry.

The world has seen a steep decrease in cost and it has been predicted that the costs will drop by 66% by 2040.[298] These predictions are based on the silicon-based solar cells, while generally accepted that PSCs are low cost. The life cycle of a solar cell was divided into four parts, from raw material, module fabrication, module operation, and disposal, which is the cradle-to-grave lifetime for electronic devices.[302] Lifecycle are more important when someone considers the real world applications and commercialization of PSCs. According to our comparative cost-performance analysis on high efficiency and moderate efficiency PSCs, to be competitive with the dominating c-Si PV (PCE of 21%), the levelized cost of electricity (LCOE) of perovskite PV has to hit 5.50 US cent kWh^{-1}. Therefore, we suggest that lifetime of 15 years is the threshold for perovskite PV (with a PCE of 19% and module size of at least 100 cm^2), which is a long way to go from current status.[303] Studies related to long-term stability is still limited.[304] Transparent conductive electrodes are ITO or FTO substrates and are the most expensive element of perovskite solar modules.[305] In another report, the analysis showed that even if the cost of the active layers and rear electrode were reduced to zero, a module PCE of 18% and a lifetime of 20 years would be required to meet the 9 US cents kWh^{-1} target.[306]

8. Conclusion

In conclusion, along with the astounding progress in the efficiency of perovskite solar cells, researches on the issue of instability have attracted enormous attention. To allow the perovskite solar cells to be commercialized, instability of device is one of the main barriers that have to be first overcome in the laboratory. Although the stability of perovskite has been improved from several minutes to thousands of hours, its improvement is not good enough for practical applications; we should extend the lifetime of perovskite solar cell to more than ten years for commercialization. Various degradation mechanisms have been proposed for perovskite solar cells, which provide a fundamental understanding and some awareness for stability enhancement. In order to enhance the stability of the perovskites, a number of factors must be taken into account for their systematic engineering, including structure design, charge transport materials, electrode material preparation, and encapsulation methods. Encapsulation plays a vital role in improving the stability of perovskite solar cells that will help to accelerate the technology to the goal of commercialization. To attain the great goal concerning efficiency as well as stability just modifying the current perovskite materials or interface is not enough; we recommend developing some new materials and designs with high stability in severe conditions. We

conclude that this may be the key point of future development of perovskite solar cells.

Acknowledgements

R.W. and M.M. contributed equally to this work. Y.Y. acknowledges the Air Force Office of Scientific Research (AFOSR) (grant no. FA2386-18-1-4094), the Office of Naval Research (ONR) (grant no. N00014-17-1-2,484), and the UC Solar Program (grant no. MRPI 328368) for their financial support. Y.D. acknowledges the National Natural Science Foundation of China (Grant Nos. 61675088) and International Science & Technology Cooperation Program of Jilin (Grant Nos.20190701023GH) for financial support. Z.K.W. acknowledges the National Key R&D Program of China (No. 2016YFA0202400) for financial support.

Conflict of Interest

The authors declare no conflict of interest.

Keywords

degradation, perovskite solar cells, stability

Received: December 12, 2018
Revised: January 13, 2019
Published online:

[1] a) S. N. Habisreutinger, T. Leijtens, G. E. Eperon, S. D. Stranks, R. J. Nicholas, H. J. Snaith, *Nano Lett.* **2014**, *14*, 5561; b) J. S. Shaikh, N. S. Shaikh, A. D. Sheikh, S. S. Mali, A. J. Kale, P. Kanjanaboos, C. K. Hong, J. H. Kim, P. S. Patil, *Mater. Des.* **2017**, *136*, 54.

[2] J. Yan, B. R. Saunders, *RSC Adv.* **2014**, *4*, 43286.

[3] S. Gholipour, M. Saliba, *Small* **2018**, *14*, 1802385.

[4] a) W. C. Chang, D. H. Lan, K. M. Lee, X. F. Wang, C. L. Liu, *ChemSusChem* **2017**, *10*, 1405; b) Z. Liang, S. Zhang, X. Xu, N. Wang, J. Wang, X. Wang, Z. Bi, G. Xu, N. Yuan, J. Ding, *RSC Adv.* **2015**, *5*, 60562; c) D. K. Mohamad, J. Griffin, C. Bracher, A. T. Barrows, D. G. Lidzey, *Adv. Energy Mater.* **2016**, *6*, 1600994.

[5] a) J. Burschka, N. Pellet, S. J. Moon, R. Humphry-Baker, P. Gao, M. K. Nazeeruddin, M. Gratzel, *Nature* **2013**, *499*, 316; b) L. Huang, C. Li, X. Sun, R. Xu, Y. Du, J. Ni, H. Cai, J. Li, Z. Hu, J. Zhang, *Org. Electron.* **2017**, *40*, 13.

[6] Z. Xiao, C. Bi, Y. Shao, Q. Dong, Q. Wang, Y. Yuan, C. Wang, Y. Gao, J. Huang, *Energy Environ. Sci.* **2014**, *7*, 2619.

[7] P. Luo, Z. Liu, W. Xia, C. Yuan, J. Cheng, Y. Lu, *J. Mater. Chem. A* **2015**, *3*, 12443.

[8] M. R. Leyden, M. V. Lee, S. R. Raga, Y. Qi, *J. Mater. Chem. A* **2015**, *3*, 16097.

[9] a) Z. Wei, H. Chen, K. Yan, S. Yang, *Angew. Chem., Int. Ed.* **2014**, *53*, 13239; b) M. M. Lee, J. Teuscher, T. Miyasaka, T. N. Murakami, H. J. Snaith, *Science* **2012**, *338*, 643; c) S.-G. Li, K.-J. Jiang, M.-J. Su, X.-P. Cui, J.-H. Huang, Q.-Q. Zhang, X.-Q. Zhou, L.-M. Yang, Y.-L. Song, *J. Mater. Chem. A* **2015**, *3*, 9092.

[10] a) K. Hwang, Y. S. Jung, Y. J. Heo, F. H. Scholes, S. E. Watkins, J. Subbiah, D. J. Jones, D. Y. Kim, D. Vak, *Adv. Mater.* **2015**, *27*, 1241; b) S. Tang, Y. Deng, X. Zheng, Y. Bai, Y. Fang, Q. Dong, H. Wei, J. Huang, *Adv. Energy Mater.* **2017**, *7*, 1700302; c) M. Yang, Z. Li, M. O. Reese, O. G. Reid, D. H. Kim, S. Siol, T. R. Klein, Y. Yan, J. J. Berry, M. F. A. M. van Hest, K. Zhu, *Nat. Energy* **2017**, *2*, 17038.

[11] a) A. Mei, X. Li, L. Liu, Z. Ku, T. Liu, Y. Rong, M. Xu, M. Hu, J. Chen, Y. Yang, M. Gratzel, H. Han, *Science* **2014**, *345*, 295; b) Z. Ku, Y. Rong, M. Xu, T. Liu, H. Han, *Sci. Rep.* **2013**, *3*, 3132.

[12] Y. Liu, Z. Yang, D. Cui, X. Ren, J. Sun, X. Liu, J. Zhang, Q. Wei, H. Fan, F. Yu, X. Zhang, C. Zhao, S. F. Liu, *Adv. Mater.* **2015**, *27*, 5176.

[13] T. Baikie, Y. Fang, J. M. Kadro, M. Schreyer, F. Wei, S. G. Mhaisalkar, M. Graetzel, T. J. White, *J. Mater. Chem. A* **2013**, *1*, 5628.

[14] V. D'Innocenzo, G. Grancini, M. J. Alcocer, A. R. Kandada, S. D. Stranks, M. M. Lee, G. Lanzani, H. J. Snaith, A. Petrozza, *Nat. Commun.* **2014**, *5*, 3586.

[15] J. R. Poindexter, R. L. Z. Hoye, L. Nienhaus, R. C. Kurchin, A. E. Morishige, E. E. Looney, A. Osherov, J. P. Correa-Baena, B. Lai, V. Bulovic, V. Stevanovic, M. G. Bawendi, T. Buonassisi, *ACS Nano* **2017**, *11*, 7101.

[16] E. Klampaftis, B. S. Richards, *Prog. Photovoltaics* **2011**, *19*, 345.

[17] a) Y. Yang, J. Wu, T. Wu, Z. Xu, X. Liu, Q. Guo, X. He, *J. Colloid Interface Sci.* **2018**, *531*, 602; b) L. J. Zuo, H. X. Guo, D. W. deQuilettes, S. Jariwala, N. De Marco, S. Q. Dong, R. DeBlock, D. S. Ginger, B. Dunn, M. K. Wang, Y. Yang, *Sci Adv* **2017**, *3*, e1700106; c) X. Zheng, Z. Wei, H. Chen, Y. Bai, S. Xiao, T. Zhang, S. Yang, *J. Energy Chem.* **2015**, *24*, 736; d) P. W. Liang, C. Y. Liao, C. C. Chueh, F. Zuo, S. T. Williams, X. K. Xin, J. Lin, A. K. Jen, *Adv. Mater.* **2014**, *26*, 3748.

[18] a) M. A. Green, K. Emery, Y. Hishikawa, W. Warta, E. D. Dunlop, *Prog. Photovoltaics* **2015**, *23*, 1; b) B. O'Regan, M. A. Gratzel, *Nature* **1991**, *353*, 737.

[19] U. Bach, D. Lupo, P. Comte, J. E. Moser, F. Weissörtel, J. Salbeck, H. Spreitzer, M. Gratzel, *Nature* **1998**, *395*, 583.

[20] a) J. Krüger, R. Plass, L. Cevey, M. Piccirelli, M. Grätzel, U. Bach, *Appl. Phys. Lett.* **2001**, *79*, 2085; b) J. Krüger, R. Plass, M. Grätzel, H.-J. Matthieu, *Appl. Phys. Lett.* **2002**, *81*, 367; c) L. Schmidt-Mende, S. M. Zakeeruddin, M. Grätzel, *Appl. Phys. Lett.* **2005**, *86*, 013504; d) H. J. Snaith, R. Humphry-Baker, P. Chen, I. Cesar, S. M. Zakeeruddin, M. Gratzel, *Nanotechnology* **2008**, *19*, 424003.

[21] H. S. Kim, C. R. Lee, J. H. Im, K. B. Lee, T. Moehl, A. Marchioro, S. J. Moon, R. Humphry-Baker, J. H. Yum, J. E. Moser, M. Gratzel, N. G. Park, *Sci. Rep.* **2012**, *2*, 591.

[22] L. Etgar, P. Gao, Z. Xue, Q. Peng, A. K. Chandiran, B. Liu, M. K. Nazeeruddin, M. Gratzel, *J. Am. Chem. Soc.* **2012**, *134*, 17396.

[23] J. M. Ball, M. M. Lee, A. Hey, H. J. Snaith, *Energy Environ. Sci.* **2013**, *6*, 1739.

[24] a) W. S. Yang, J. H. Noh, N. J. Jeon, Y. C. Kim, S. Ryu, J. Seo, S. I. Seok, *Science* **2015**, *348*, 1234; b) N. J. Jeon, J. H. Noh, W. S. Yang, Y. C. Kim, S. Ryu, J. Seo, S. I. Seok, *Nature* **2015**, *517*, 476.

[25] M. Li, C. Zhao, Z.-K. Wang, C.-C. Zhang, H. K. H. Lee, A. Pockett, J. Barbé, W. C. Tsoi, Y.-G. Yang, M. J. Carnie, X.-Y. Gao, W.-X. Yang, J. R. Durrant, L.-S. Liao, S. M. Jain, *Adv. Energy Mater.* **2018**, *8*, 1801509.

[26] S. R. Raga, M.-C. Jung, M. V. Lee, M. R. Leyden, Y. Kato, Y. Qi, *Chem. Mater.* **2015**, *27*, 1597.

[27] J. A. Christians, P. A. Miranda Herrera, P. V. Kamat, *J. Am. Chem. Soc.* **2015**, *137*, 1530.

[28] H. P. Zhou, Q. Chen, G. Li, S. Luo, T. B. Song, H. S. Duan, Z. R. Hong, J. B. You, Y. S. Liu, Y. Yang, *Science* **2014**, *345*, 542.

[29] K. K. Bass, R. E. McAnally, S. Zhou, P. I. Djurovich, M. E. Thompson, B. C. Melot, *Chem. Commun.* **2014**, *50*, 15819.

[30] W. Li, J. Fan, Y. Mai, L. Wang, *Adv. Energy Mater.* **2017**, *7*, 1601433.

[31] P. Rajput, G. N. Tiwari, O. S. Sastry, B. Bora, V. Sharma, *Sol. Energy* **2016**, *135*, 786.
[32] a) M. Liu, M. B. Johnston, H. J. Snaith, *Nature* **2013**, *501*, 395; b) Q. Fu, X. Tang, B. Huang, T. Hu, L. Tan, L. Chen, Y. Chen, *Adv. Sci.* **2018**, *5*, 1700387; c) D. M. Tanenbaum, H. F. Dam, R. Rösch, M. Jørgensen, H. Hoppe, F. C. Krebs, *Sol. Energy Mater. Sol. Cells* **2012**, *97*, 157.
[33] B. J. Kim, S. Lee, H. S. Jung, *J. Mater. Chem. A* **2018**, *6*, 12215.
[34] a) J. Y. Kim, *Key Eng. Mater.* **2017**, *753*, 156; b) J. Ma, J. Chang, Z. Lin, X. Guo, L. Zhou, Z. Liu, H. Xi, D. Chen, C. Zhang, Y. Hao, *J. Phys. Chem. C* **2018**, *122*, 1044.
[35] a) H. Dong, S. Pang, Y. Zhang, D. Chen, W. Zhu, H. Xi, J. Chang, J. Zhang, C. Zhang, Y. Hao, *Nanomaterials* **2018**, *8*, E720; b) S. Pang, X. Li, H. Dong, D. Chen, W. Zhu, J. Chang, Z. Lin, H. Xi, J. Zhang, C. Zhang, Y. Hao, *ACS Appl. Mater. Interfaces* **2018**, *10*, 12731; c) X. Sun, C. Zhang, J. Chang, H. Yang, H. Xi, G. Lu, D. Chen, Z. Lin, X. Lu, J. Zhang, Y. Hao, *Nano Energy* **2016**, *28*, 417.
[36] L. Meng, C. Sun, R. Wang, W. Huang, Z. Zhao, P. Sun, T. Huang, J. Xue, J. W. Lee, C. Zhu, Y. Huang, Y. Li, Y. Yang, *J. Am. Chem. Soc.* **2018**, *140*, 17255.
[37] a) M. Gratzel, *Acc. Chem. Res.* **2009**, *42*, 1788; b) M. Grätzel, *Chem. Lett.* **2005**, *34*, 8.
[38] a) C. Grätzel, S. M. Zakeeruddin, *Mater. Today* **2013**, *16*, 11; b) B. E. Hardin, H. J. Snaith, M. D. McGehee, *Nat. Photonics* **2012**, *6*, 162; c) A. Hagfeldt, G. Boschloo, L. Sun, L. Kloo, H. Pettersson, *Chem. Rev.* **2010**, *110*, 6595.
[39] A. Mei, X. Li, L. Liu, Z. Ku, T. Liu, Y. Rong, M. Xu, M. Hu, J. C. Chen, Y. Yang, M. Grätzel, H. Han, *Science* **2014**, *345*, 295.
[40] a) S. Mathew, A. Yella, P. Gao, R. Humphry-Baker, B. F. Curchod, N. Ashari-Astani, I. Tavernelli, U. Rothlisberger, M. K. Nazeeruddin, M. Gratzel, *Nat. Chem.* **2014**, *6*, 242; b) J. H. Noh, S. H. Im, J. H. Heo, T. N. Mandal, S. I. Seok, *Nano Lett.* **2013**, *13*, 1764.
[41] K. Wojciechowski, M. Saliba, T. Leijtens, A. Abate, H. J. Snaith, *Energy Environ. Sci.* **2014**, *7*, 1142.
[42] B. Conings, L. Baeten, C. De Dobbelaere, J. D'Haen, J. Manca, H. G. Boyen, *Adv. Mater.* **2014**, *26*, 2041.
[43] W. Liu, Y. Zhang, *J. Mater. Chem. A* **2014**, *2*, 10244.
[44] A. Yella, L. P. Heiniger, P. Gao, M. K. Nazeeruddin, M. Gratzel, *Nano Lett.* **2014**, *14*, 2591.
[45] S. Shi, Y. Li, X. Li, H. Wang, *Mater. Horiz.* **2015**, *2*, 378.
[46] J. T. Wang, J. M. Ball, E. M. Barea, A. Abate, J. A. Alexander-Webber, J. Huang, M. Saliba, I. Mora-Sero, J. Bisquert, H. J. Snaith, R. J. Nicholas, *Nano Lett.* **2014**, *14*, 724.
[47] a) Z. Liu, M. Zhang, X. Xu, L. Bu, W. Zhang, W. Li, Z. Zhao, M. Wang, Y. B. Cheng, H. He, *Dalton Trans.* **2015**, *44*, 3967; b) X. Xu, Z. Liu, Z. Zuo, M. Zhang, Z. Zhao, Y. Shen, H. Zhou, Q. Chen, Y. Yang, M. Wang, *Nano Lett.* **2015**, *15*, 2402.
[48] F. Di Giacomo, V. Zardetto, A. D'Epifanio, S. Pescetelli, F. Matteocci, S. Razza, A. Di Carlo, S. Licoccia, W. M. M. Kessels, M. Creatore, T. M. Brown, *Adv. Energy Mater.* **2015**, *5*, 1401808.
[49] L. Liang, Z. Huang, L. Cai, W. Chen, B. Wang, K. Chen, H. Bai, Q. Tian, B. Fan, *ACS Appl. Mater. Interfaces* **2014**, *6*, 20585.
[50] S. Dharani, H. K. Mulmudi, N. Yantara, P. T. Thu Trang, N. G. Park, M. Graetzel, S. Mhaisalkar, N. Mathews, P. P. Boix, *Nanoscale* **2014**, *6*, 1675.
[51] T. Leijtens, B. Lauber, G. E. Eperon, S. D. Stranks, H. J. Snaith, *J. Phys. Chem. Lett.* **2014**, *5*, 1096.
[52] H. S. Kim, N. G. Park, *J. Phys. Chem. Lett.* **2014**, *5*, 2927.
[53] A. Kojima, K. Teshima, Y. Shirai, T. Miyasaka, *J. Am. Chem. Soc.* **2009**, *131*, 6050.
[54] J. H. Heo, S. H. Im, J. H. Noh, T. N. Mandal, C.-S. Lim, J. A. Chang, Y. H. Lee, H.-j. Kim, A. Sarkar, M. K. Nazeeruddin, M. Grätzel, S. I. Seok, *Nat. Photonics* **2013**, *7*, 486.
[55] K. Mahmood, B. S. Swain, H. S. Jung, *Nanoscale* **2014**, *6*, 9127.
[56] K. Mahmood, R. Munir, B. S. Swain, G.-S. Han, B.-J. Kim, H. S. Jung, *RSC Adv.* **2014**, *4*, 9072.
[57] a) I. C. Smith, E. T. Hoke, D. Solis-Ibarra, M. D. McGehee, H. I. Karunadasa, *Angew. Chem., Int. Ed.* **2014**, *53*, 11232; b) J.-W. Lee, D.-H. Kim, H.-S. Kim, S.-W. Seo, S. M. Cho, N.-G. Park, *Adv. Energy Mater.* **2015**, *5*, 1501310; c) X. Li, M. I. Dar, C. Yi, J. Luo, M. Tschumi, S. M. Zakeeruddin, M. K. Nazeeruddin, H. Han, M. Gratzel, *Nat. Chem.* **2015**, *7*, 703.
[58] M. Saliba, T. Matsui, J. Y. Seo, K. Domanski, J. P. Correa-Baena, M. K. Nazeeruddin, S. M. Zakeeruddin, W. Tress, A. Abate, A. Hagfeldt, M. Gratzel, *Energy Environ. Sci.* **2016**, *9*, 1989.
[59] a) T. Matsui, J. Y. Seo, M. Saliba, S. M. Zakeeruddin, M. Gratzel, *Adv. Mater.* **2017**, *29*, 1606258 b) N. J. Jeon, J. H. Noh, Y. C. Kim, W. S. Yang, S. Ryu, S. I. Seok, *Nat. Mater.* **2014**, *13*, 897; c) J. B. You, Z. R. Hong, Y. Yang, Q. Chen, M. Cai, T. B. Song, C. C. Chen, S. R. Lu, Y. S. Liu, H. P. Zhou, Y. Yang, *ACS Nano* **2014**, *8*, 1674.
[60] L. Yang, A. T. Barrows, D. G. Lidzey, T. Wang, *Rep. Prog. Phys.* **2016**, *79*, 026501.
[61] a) K. Sun, J. Chang, F. H. Isikgor, P. Li, J. Ouyang, *Nanoscale* **2015**, *7*, 896; b) J. Min, Z.-G. Zhang, Y. Hou, C. O. Ramirez Quiroz, T. Przybilla, C. Bronnbauer, F. Guo, K. Forberich, H. Azimi, T. Ameri, E. Spiecker, Y. Li, C. J. Brabec, *Chem. Mater.* **2015**, *27*, 227.
[62] a) Y. Cai, Z. Zhang, Y. Zhou, H. Liu, Q. Qin, X. Lu, X. Gao, L. Shui, S. Wu, J. Liu, *Electrochim. Acta* **2018**, *261*, 445; b) Z. Liu, J. Hu, H. Jiao, L. Li, G. Zheng, Y. Chen, Y. Huang, Q. Zhang, C. Shen, Q. Chen, H. Zhou, *Adv. Mater.* **2017**, *29*, 1606774.
[63] H. Dong, Z. Wu, J. Xi, X. Xu, L. Zuo, T. Lei, X. Zhao, L. Zhang, X. Hou, A. K. Y. Jen, *Adv. Funct. Mater.* **2018**, *28*, 1704836.
[64] F. Xie, C.-C. Chen, Y. Wu, X. Li, M. Cai, X. Liu, X. Yang, L. Han, *Energy Environ. Sci.* **2017**, *10*, 1942.
[65] Y. Zheng, J. Kong, D. Huang, W. Shi, L. McMillon-Brown, H. E. Katz, J. Yu, A. D. Taylor, *Nanoscale* **2018**, *10*, 11342.
[66] a) Y. Zheng, W. Shi, J. Kong, D. Huang, H. E. Katz, J. Yu, A. D. Taylor, *Small Methods* **2017**, *1*, 1700244; b) Y. Hou, X. Y. Du, S. Scheiner, D. P. McMeekin, Z. P. Wang, N. Li, M. S. Killian, H. W. Chen, M. Richter, I. Levchuk, N. Schrenker, E. Spiecker, T. Stubhan, N. A. Luechinger, A. Hirsch, P. Schmuki, H. P. Steinruck, R. H. Fink, M. Halik, H. J. Snaith, C. J. Brabec, *Science* **2017**, *358*, 1192.
[67] a) X. Huang, K. Wang, C. Yi, T. Meng, X. Gong, *Adv. Energy Mater.* **2016**, *6*, 1501773; b) J. Huang, K.-X. Wang, J.-J. Chang, Y.-Y. Jiang, Q.-S. Xiao, Y. Li, *J. Mater. Chem. A* **2017**, *5*, 13817.
[68] P. Fan, D. Zheng, Y. Zheng, J. Yu, *Electrochim. Acta* **2018**, *283*, 922.
[69] D. Akin Kara, K. Kara, G. Oylumluoglu, M. Z. Yigit, M. Can, J. J. Kim, E. K. Burnett, D. L. Gonzalez Arellano, S. Buyukcelebi, F. Ozel, O. Usluer, A. L. Briseno, M. Kus, *ACS Appl. Mater. Interfaces* **2018**, *10*, 30000.
[70] a) J.-Y. Seo, T. Matsui, J. Luo, J.-P. Correa-Baena, F. Giordano, M. Saliba, K. Schenk, A. Ummadisingu, K. Domanski, M. Hadadian, A. Hagfeldt, S. M. Zakeeruddin, U. Steiner, M. Grätzel, A. Abate, *Adv. Energy Mater.* **2016**, *6*, 1600767; b) D. Luo, W. Yang, Z. Wang, A. Sadhanala, Q. Hu, R. Su, R. Shivanna,G. F. Trindade, J. F. Watts, Z. Xu, T. Liu, K. Chen, F. Ye, P. Wu,L. Zhao, J. Wu, Y. Tu, Y. Zhang, X. Yang, W. Zhang, R. H. Friend, Q. Gong, H. J. Snaith, R. Zhu, *Science* **2018**, *360*, 1442.
[71] E. H. Anaraki, A. Kermanpur, L. Steier, K. Domanski, T. Matsui, W. Tress, M. Saliba, A. Abate, M. Grätzel, A. Hagfeldt, J.-P. Correa-Baena, *Energy Environ. Sci.* **2016**, *9*, 3128.
[72] a) Q. Jiang, Z. Chu, P. Wang, X. Yang, H. Liu, Y. Wang, Z. Yin, J. Wu, X. Zhang, J. You, *Adv. Mater.* **2017**, *29*, 1703852; b) Q. Jiang,

L. Zhang, H. Wang, X. Yang, J. Meng, H. Liu, Z. Yin, J. Wu, X. Zhang, J. You, *Nat. Energy* **2017**, *2*, 16177.
[73] W. S. Yang, B-W Park, E. H. Jung, N. J. Jeon, D. U. Lee, S. S. Shin, J. Seo, E. K. Kim, J. H. Noh, S. I. Seok, *Science* **2017**, *356*, 1376.
[74] M. Saliba, J.-P. Correa-Baena, C. M. Wolff, M. Stolterfoht, N. Phung, S. Albrecht, D. Neher, A. Abate, *Chem. Mater.* **2018**, *30*, 4193.
[75] a) Y. Wu, X. Yang, W. Chen, Y. Yue, M. Cai, F. Xie, E. Bi, A. Islam, L. Han, *Nat. Energy* **2016**, *1*, 16148; b) J. You, L. Meng, T. B. Song, T. F. Guo, Y. M. Yang, W. H. Chang, Z. Hong, H. Chen, H. Zhou, Q. Chen, Y. Liu, N. De Marco, Y. Yang, *Nat. Nanotechnol.* **2016**, *11*, 75.
[76] a) I. J. Park, G. Kang, M. A. Park, J. S. Kim, S. W. Seo, D. H. Kim, K. Zhu, T. Park, J. Y. Kim, *ChemSusChem* **2017**, *10*, 2660; b) Y. Shao, Y. Yuan, J. Huang, *Nat. Energy* **2016**, *1*, 15001; c) W. Chen, Y. Z. Wu, Y. F. Yue, J. Liu, W. J. Zhang, X. D. Yang, H. Chen, E. B. Bi, I. Ashraful, M. Gratzel, L. Y. Han, *Science* **2015**, *350*, 944.
[77] X. Crispin, F. L. E. Jakobsson, A. Crispin, P. C. M. Grim, P. Andersson, A. Volodin, C. van Haesendonck, M. Van der Auweraer, W. R. Salaneck, M. Berggren, *Chem. Mater.* **2006**, *18*, 4354.
[78] a) S. Sun, T. Salim, N. Mathews, M. Duchamp, C. Boothroyd, G. Xing, T. C. Sum, Y. M. Lam, *Energy Environ. Sci.* **2014**, *7*, 399; b) P. Docampo, J. M. Ball, M. Darwich, G. E. Eperon, H. J. Snaith, *Nat. Commun.* **2013**, *4*, 2761.
[79] J. Y. Jeng, Y. F. Chiang, M. H. Lee, S. R. Peng, T. F. Guo, P. Chen, T. C. Wen, *Adv. Mater.* **2013**, *25*, 3727.
[80] J. H. Heo, H. J. Han, D. Kim, T. K. Ahn, S. H. Im, *Energy Environ. Sci.* **2015**, *8*, 1602.
[81] Q. Wang, C. C. Chueh, M. Eslamian, A. K. Jen, *ACS Appl. Mater. Interfaces* **2016**, *8*, 32068.
[82] L. Hu, K. Sun, M. Wang, W. Chen, B. Yang, J. Fu, Z. Xiong, X. Li, X. Tang, Z. Zang, S. Zhang, L. Sun, M. Li, *ACS Appl. Mater. Interfaces* **2017**, *9*, 43902.
[83] H. Yang, J. Zhang, C. Zhang, J. Chang, Z. Lin, D. Chen, X. Sun, H. Xi, G. Han, Y. Hao, *Sol. Energy* **2016**, *139*, 190.
[84] C.-H. Chiang, Z.-L. Tseng, C.-G. Wu, *J. Mater. Chem. A* **2014**, *2*, 15897.
[85] K. W. Wong, H. L. Yip, Y. Luo, K. Y. Wong, W. M. Lau, K. H. Low, H. F. Chow, Z. Q. Gao, W. L. Yeung, C. C. Chang, *Appl. Phys. Lett.* **2002**, *80*, 2788.
[86] H. Choi, C. K. Mai, H. B. Kim, J. Jeong, S. Song, G. C. Bazan, J. Y. Kim, A. J. Heeger, *Nat. Commun.* **2015**, *6*, 7348.
[87] D. Lee, H. Lee, Y. Ahn, Y. Lee, *Carbon* **2015**, *81*, 439.
[88] A. Agresti, S. Pescetelli, B. Taheri, A. E. Del Rio Castillo, L. Cina, F. Bonaccorso, A. Di Carlo, *ChemSusChem* **2016**, *9*, 2609.
[89] Q.-D. Yang, J. Li, Y. Cheng, H.-W. Li, Z. Guan, B. Yu, S.-W. Tsang, *J. Mater. Chem. A* **2017**, *5*, 9852.
[90] J.-S. Yeo, R. Kang, S. Lee, Y.-J. Jeon, N. Myoung, C.-L. Lee, D.-Y. Kim, J.-M. Yun, Y.-H. Seo, S.-S. Kim, S.-I. Na, *Nano Energy* **2015**, *12*, 96.
[91] J. M. Kim, C. W. Jang, J. H. Kim, S. Kim, S.-H. Choi, *Appl. Surf. Sci.* **2018**, *455*, 1131.
[92] T. H. Chowdhury, M. Akhtaruzzaman, M. E. Kayesh, R. Kaneko, T. Noda, J.-J. Lee, A. Islam, *Sol. Energy* **2018**, *171*, 652.
[93] J.-S. Yeo, C.-H. Lee, D. Jang, S. Lee, S. M. Jo, H.-I. Joh, D.-Y. Kim, *Nano Energy* **2016**, *30*, 667.
[94] Z. Zhou, X. Li, M. Cai, F. Xie, Y. Wu, Z. Lan, X. Yang, Y. Qiang, A. Islam, L. Han, *Adv. Energy Mater.* **2017**, *7*, 1700763.
[95] Q. Wang, Y. Shao, Q. Dong, Z. Xiao, Y. Yuan, J. Huang, *Energy Environ. Sci.* **2014**, *7*, 2359.
[96] L. Q. Zhang, X. W. Zhang, Z. G. Yin, Q. Jiang, X. Liu, J. H. Meng, Y. J. Zhao, H. L. Wang, *J. Mater. Chem. A* **2015**, *3*, 12133.
[97] C. Sun, Z. Wu, H.-L. Yip, H. Zhang, X.-F. Jiang, Q. Xue, Z. Hu, Z. Hu, Y. Shen, M. Wang, F. Huang, Y. Cao, *Adv. Energy Mater.* **2016**, *6*, 1501534.
[98] C. Tian, E. Castro, G. Betancourt-Solis, Z. Nan, O. Fernandez-Delgado, S. Jankuru, L. Echegoyen, *New J. Chem.* **2018**, *42*, 2896.
[99] H. I. Kim, M.-J. Kim, K. Choi, C. Lim, Y.-H. Kim, S.-K. Kwon, T. Park, *Adv. Energy Mater.* **2018**, *8*, 1702872.
[100] R. Lindblad, D. Bi, B. W. Park, J. Oscarsson, M. Gorgoi, H. Siegbahn, M. Odelius, E. M. Johansson, H. Rensmo, *J. Phys. Chem. Lett.* **2014**, *5*, 648.
[101] S. Bao, J. Wu, X. He, Y. Tu, S. Wang, M. Huang, Z. Lan, *Electrochim. Acta* **2017**, *251*, 307.
[102] J. Jia, J. Wu, J. Dong, L. Fan, M. Huang, J. Lin, Z. Lan, *Chem. Commun.* **2018**, *54*, 3170.
[103] X. Liu, Z. Liu, H. Ye, Y. Tu, B. Sun, X. Tan, T. Shi, Z. Tang, G. Liao, *Electrochim. Acta* **2018**, *288*, 115.
[104] I. Jeon, S. Seo, Y. Sato, C. Delacou, A. Anisimov, K. Suenaga, E. I. Kauppinen, S. Maruyama, Y. Matsuo, *J. Phys. Chem. C* **2017**, *121*, 25743.
[105] Y. Zhou, X. Yin, Q. Luo, X. Zhao, D. Zhou, J. Han, F. Hao, M. Tai, J. Li, P. Liu, K. Jiang, H. Lin, *ACS Appl. Mater. Interfaces* **2018**, *10*, 31384.
[106] K. Aitola, K. Domanski, J. P. Correa-Baena, K. Sveinbjornsson, M. Saliba, A. Abate, M. Gratzel, E. Kauppinen, E. M. J. Johansson, W. Tress, A. Hagfeldt, G. Boschloo, *Adv. Mater.* **2017**, *29*, 1606398.
[107] a) G. Niu, W. Li, F. Meng, L. Wang, H. Dong, Y. Qiu, *J. Mater. Chem. A* **2014**, *2*, 705; b) S. Ito, S. Tanaka, K. Manabe, H. Nishino, *J. Phys. Chem. C* **2014**, *118*, 16995; c) W. Li, H. Dong, L. Wang, N. Li, X. Guo, J. Li, Y. Qiu, *J. Mater. Chem. A* **2014**, *2*, 13587; d) M. Zhang, S. Dai, S. Chandrabose, K. Chen, K. Liu, M. Qin, X. Lu, J. M. Hodgkiss, H. Zhou, X. Zhan, *J. Am. Chem. Soc.* **2018**, *140*, 14938; e) M. Qin, J. Cao, T. Zhang, J. Mai, T.-K. Lau, S. Zhou, Y. Zhou, J. Wang, Y.-J. Hsu, N. Zhao, J. Xu, X. Zhan, X. Lu, *Adv. Energy Mater.* **2018**, *8*, 1703399.
[108] J. L. Yang, B. D. Siempelkamp, D. Y. Liu, T. L. Kelly, *ACS Nano* **2015**, *9*, 1955.
[109] B. Conings, J. Drijkoningen, N. Gauquelin, A. Babayigit, J. D'Haen, L. D'Olieslaeger, A. Ethirajan, J. Verbeeck, J. Manca, E. Mosconi, F. D. Angelis, H.-G. Boyen, *Adv. Energy Mater.* **2015**, *5*, 1500477.
[110] Y. Chen, Y. Sun, J. Peng, J. Tang, K. Zheng, Z. Liang, *Adv. Mater.* **2018**, *30*, 1703487.
[111] a) B. Brunetti, C. Cavallo, A. Ciccioli, G. Gigli, A. Latini, *Sci. Rep.* **2016**, *6*, 31896; b) H. Cho, Y. H. Kim, C. Wolf, H. D. Lee, T. W. Lee, *Adv. Mater.* **2018**, *30*, 1704587.
[112] B. Roose, K. C. Gödel, S. Pathak, A. Sadhanala, J. P. C. Baena, B. D. Wilts, H. J. Snaith, U. Wiesner, M. Grätzel, U. Steiner, A. Abate, *Adv. Energy Mater.* **2016**, *6*, 1501868.
[113] Y. S. Kwon, J. Lim, H.-J. Yun, Y.-H. Kim, T. Park, *Energy Environ. Sci.* **2014**, *7*, 1454.
[114] B. Philippe, B.-W. Park, R. Lindblad, J. Oscarsson, S. Ahmadi, E. M. J. Johansson, H. Rensmo, *Chem. Mater.* **2015**, *27*, 1720.
[115] J. Liu, Y. Wu, C. Qin, X. Yang, T. Yasuda, A. Islam, K. Zhang, W. Peng, W. Chen, L. Han, *Energy Environ. Sci.* **2014**, *7*, 2963.
[116] a) C. Yi, J. Luo, S. Meloni, A. Boziki, N. Ashari-Astani, C. Grätzel, S. M. Zakeeruddin, U. Röthlisberger, M. Grätzel, *Energy Environ. Sci.* **2016**, *9*, 656; b) D. Q. Bi, W. Tress, M. I. Dar, P. Gao, J. S. Luo, C. Renevier, K. Schenk, A. Abate, F. Giordano, J. P. C. Baena, J. D. Decoppet, S. M. Zakeeruddin, M. K. Nazeeruddin, M. Gratzel, A. Hagfeldt, *Sci. Adv.* **2016**, *2*, e1501170; c) Z. Li, M. Yang, J.-S. Park, S.-H. Wei, J. J. Berry, K. Zhu, *Chem. Mater.* **2015**, *28*, 284.
[117] G. E. Eperon, S. N. Habisreutinger, T. Leijtens, B. J. Bruijnaers, J. J. van Franeker, D. W. Dequilettes, S. Pathak, R. J. Sutton, G. Grancini, D. S. Ginger, R. A. J. Janssen, A. Petrozza, H. J. Snaith, *ACS Nano* **2015**, *9*, 9380.

[118] a) A. M. A. Leguy, Y. Hu, M. Campoy-Quiles, M. I. Alonso, O. J. Weber, P. Azarhoosh, M. van Schilfgaarde, M. T. Weller, T. Bein, J. Nelson, P. Docampo, P. R. F. Barnes, *Chem. Mater.* **2015**, *27*, 3397; b) P. Docampo, T. Bein, *Acc. Chem. Res.* **2016**, *49*, 339.

[119] a) A. R. b. M. Yusoff, M. K. Nazeeruddin, *Adv. Energy Mater.* **2018**, *8*, 1702073; b) Y. Guo, K. Shoyama, W. Sato, Y. Matsuo, K. Inoue, K. Harano, C. Liu, H. Tanaka, E. Nakamura, *J. Am. Chem. Soc.* **2015**, *137*, 15907; c) A. Wakamiya, M. Endo, T. Sasamori, N. Tokitoh, Y. Ogomi, S. Hayase, Y. Murata, *Chem. Lett.* **2014**, *43*, 711.

[120] T. M. Koh, V. Shanmugam, J. Schlipf, L. Oesinghaus, P. Muller-Buschbaum, N. Ramakrishnan, V. Swamy, N. Mathews, P. P. Boix, S. G. Mhaisalkar, *Adv. Mater.* **2016**, *28*, 3653.

[121] D. H. Cao, C. C. Stoumpos, O. K. Farha, J. T. Hupp, M. G. Kanatzidis, *J. Am. Chem. Soc.* **2015**, *137*, 7843.

[122] H. Tsai, W. Nie, J. C. Blancon, C. C. Stoumpos, R. Asadpour, B. Harutyunyan, A. J. Neukirch, R. Verduzco, J. J. Crochet, S. Tretiak, L. Pedesseau, J. Even, M. A. Alam, G. Gupta, J. Lou, P. M. Ajayan, M. J. Bedzyk, M. G. Kanatzidis, *Nature* **2016**, *536*, 312.

[123] a) B. Kundys, A. Lappas, M. Viret, V. Kapustianyk, V. Rudyk, S. Semak, C. Simon, I. Bakaimi, *Phys. Rev. B* **2010**, *81*, 224434; b) K. Pradeesh, J. J. Baumberg, G. V. Prakash, *Appl. Phys. Lett.* **2009**, *95*, 173305.

[124] H. Zheng, G. Liu, L. Zhu, J. Ye, X. Zhang, A. Alsaedi, T. Hayat, X. Pan, S. Dai, *Adv. Energy Mater.* **2018**, *8*, 1800051.

[125] a) T. Zhang, M. I. Dar, G. Li, F. Xu, N. Guo, M. Grätzel, Y. Zhao, *Sci. Adv.* **2017**, *3*, e1700841; b) S. Shao, J. Liu, G. Portale, H.-H. Fang, G. R. Blake, G. H. ten Brink, L. J. A. Koster, M. A. Loi, *Adv. Energy Mater.* **2018**, *8*, 1702019; c) Z. Wang, Q. Lin, F. P. Chmiel, N. Sakai, L. M. Herz, H. J. Snaith, *Nat. Energy* **2017**, *2*, 17135; d) G. Grancini, C. Roldan-Carmona, I. Zimmermann, E. Mosconi, X. Lee, D. Martineau, S. Narbey, F. Oswald, F. De Angelis, M. Graetzel, M. K. Nazeeruddin, *Nat. Commun.* **2017**, *8*, 15684.

[126] D.-Y. Son, J.-W. Lee, Y. J. Choi, I.-H. Jang, S. Lee, P. J. Yoo, H. Shin, N. Ahn, M. Choi, D. Kim, N.-G. Park, *Nat. Energy* **2016**, *1*, 16081.

[127] N. Li, Z. Zhu, C.-C. Chueh, H. Liu, B. Peng, A. Petrone, X. Li, L. Wang, A. K. Y. Jen, *Adv. Energy Mater.* **2017**, *7*, 1601307.

[128] J. Fan, Y. Ma, C. Zhang, C. Liu, W. Li, R. E. I. Schropp, Y. Mai, *Adv. Energy Mater.* **2018**, *8*, 1703421.

[129] a) J. C. Blancon, H. Tsai, W. Nie, C. C. Stoumpos, L. Pedesseau, C. Katan, M. Kepenekian, C. M. M. Soe, K. Appavoo, M. Y. Sfeir, S. Tretiak, P. M. Ajayan, M. G. Kanatzidis, J. Even, J. J. Crochet, A. D. Mohite, *Science* **2017**, *355*, 1288; b) Y. Chen, Y. Sun, J. Peng, W. Zhang, X. Su, K. Zheng, T. Pullerits, Z. Liang, *Adv. Energy Mater.* **2017**, *7*, 1700162; c) C. C. Stoumpos, C. M. M. Soe, H. Tsai, W. Nie, J.-C. Blancon, D. H. Cao, F. Liu, B. Traoré, C. Katan, J. Even, A. D. Mohite, M. G. Kanatzidis, *Chem* **2017**, *2*, 427.

[130] J. Cao, C. Li, X. Lv, X. Feng, R. Meng, Y. Wu, Y. Tang, *J. Am. Chem. Soc.* **2018**, *140*, 11577.

[131] X. Yu, H. Yan, Q. Peng, *ACS Appl. Mater. Interfaces* **2018**, *10*, 28948.

[132] T. Leijtens, G. E. Eperon, S. Pathak, A. Abate, M. M. Lee, H. J. Snaith, *Nat. Commun.* **2013**, *4*, 2885.

[133] B. McKenna, J. R. Troughton, T. M. Watson, R. C. Evans, *RSC Adv.* **2017**, *7*, 32942.

[134] J. You, Y. Yang, Z. Hong, T.-B. Song, L. Meng, Y. Liu, C. Jiang, H. Zhou, W.-H. Chang, G. Li, Y. Yang, *Appl. Phys. Lett.* **2014**, *105*, 183902.

[135] H. Wei, Y. Fang, P. Mulligan, W. Chuirazzi, H.-H. Fang, C. Wang, B. R. Ecker, Y. Gao, M. A. Loi, L. Cao, J. Huang, *Nat. Photonics* **2016**, *10*, 333.

[136] Z. Wang, D. P. McMeekin, N. Sakai, S. van Reenen, K. Wojciechowski, J. B. Patel, M. B. Johnston, H. J. Snaith, *Adv. Mater.* **2017**, *29*, 1604186.

[137] J. Chen, L. Zuo, Y. Zhang, X. Lian, W. Fu, J. Yan, J. Li, G. Wu, C.-Z. Li, H. Chen, *Adv. Energy Mater.* **2018**, *8*, 1800438.

[138] a) M. Jørgensen, K. Norrman, F. C. Krebs, *Sol. Energy Mater. Sol. Cells* **2008**, *92*, 686; b) A. Hinsch, J. M. Kroon, R. Kern, I. Uhlendorf, J. Holzbock, A. Meyer, J. Ferber, *Prog. Photovoltaics* **2001**, *9*, 425.

[139] N. Aristidou, I. Sanchez-Molina, T. Chotchuangchutchaval, M. Brown, L. Martinez, T. Rath, S. A. Haque, *Angew. Chem., Int. Ed. Engl.* **2015**, *54*, 8208.

[140] D. Bryant, N. Aristidou, S. Pont, I. Sanchez-Molina, T. Chotchuna ngatchaval, S. Wheeler, J. R. Durrant, S. A. Haque, *Energy Environ. Sci.* **2016**, *9*, 1655.

[141] B. Salhi, Y. S. Wudil, M. K. Hossain, A. Al-Ahmed, F. A. Al-Sulaiman, *Renewable Sustainable Energy Rev.* **2018**, *90*, 210.

[142] S. H. Turren-Cruz, A. Hagfeldt, M. Saliba, *Science* **2018**, *362*, 449.

[143] N. Arora, M. I. Dar, A. Hinderhofer, N. Pellet, F. Schreiber, S. M. Zakeeruddin, M. Gratzel, *Science* **2017**, *358*, 768.

[144] J. Wang, Y. Chen, M. Liang, G. Ge, R. Zhou, Z. Sun, S. Xue, *Dyes Pigm.* **2016**, *125*, 399.

[145] a) Y.-Y. Zheng, G. Wu, M. Deng, H.-Z. Chen, M. Wang, B.-Z. Tang, *Thin Solid Films* **2006**, *514*, 127; b) C. Ran, J. Xu, W. Gao, C. Huang, S. Dou, *Chem. Soc. Rev.* **2018**, *47*, 4581; c) N. Ahn, K. Kwak, M. S. Jang, H. Yoon, B. Y. Lee, J. K. Lee, P. V. Pikhitsa, J. Byun, M. Choi, *Nat. Commun.* **2016**, *7*, 13422; d) X. Zheng, B. Chen, J. Dai, Y. Fang, Y. Bai, Y. Lin, H. Wei, X. C. Zeng, J. Huang, *Nat. Energy* **2017**, *2*, 17102; e) Q. Wang, B. Chen, Y. Liu, Y. Deng, Y. Bai, Q. Dong, J. Huang, *Energy Environ. Sci.* **2017**, *10*, 516.

[146] S. Huang, Z. Li, L. Kong, N. Zhu, A. Shan, L. Li, *J. Am. Chem. Soc.* **2016**, *138*, 5749.

[147] Y. Rong, L. Liu, A. Mei, X. Li, H. Han, *Adv. Energy Mater.* **2015**, *5*, 1501066.

[148] H. S. Kim, J. Y. Seo, N. G. Park, *ChemSusChem* **2016**, *9*, 2528.

[149] T. Supasai, N. Rujisamphan, K. Ullrich, A. Chemseddine, T. Dittrich, *Appl. Phys. Lett.* **2013**, *103*, 183906.

[150] a) H. B. Kim, I. Im, Y. Yoon, S. D. Sung, E. Kim, J. Kim, W. I. Lee, *J. Mater. Chem. A* **2015**, *3*, 9264; b) H. S. Rao, B. X. Chen, X. D. Wang, D. B. Kuang, C. Y. Su, *Chem. Commun.* **2017**, *53*, 5163.

[151] S. Aharon, B. E. Cohen, L. Etgar, *J. Phys. Chem. C* **2014**, *118*, 17160.

[152] T. A. Berhe, W.-N. Su, C.-H. Chen, C.-J. Pan, J.-H. Cheng, H.-M. Chen, M.-C. Tsai, L.-Y. Chen, A. A. Dubale, B.-J. Hwang, *Energy Environ. Sci.* **2016**, *9*, 323.

[153] A. Binek, F. C. Hanusch, P. Docampo, T. Bein, *J. Phys. Chem. Lett.* **2015**, *6*, 1249.

[154] a) Y. Fu, H. Zhu, A. W. Schrader, D. Liang, Q. Ding, P. Joshi, L. Hwang, X. Y. Zhu, S. Jin, *Nano Lett.* **2016**, *16*, 1000; b) Z. Wang, Z. Shi, T. Li, Y. Chen, W. Huang, *Angew. Chem., Int. Ed. Engl.* **2017**, *56*, 1190.

[155] J. W. Lee, D. J. Seol, A. N. Cho, N. G. Park, *Adv. Mater.* **2014**, *26*, 4991.

[156] K. A. Bush, A. F. Palmstrom, Z. J. Yu, M. Boccard, R. Cheacharoen, J. P. Mailoa, D. P. McMeekin, R. L. Z. Hoye, C. D. Bailie, T. Leijtens, I. M. Peters, M. C. Minichetti, N. Rolston, R. Prasanna, S. Sofia, D. Harwood, W. Ma, F. Moghadam, H. J. Snaith, T. Buonassisi, Z. C. Holman, S. F. Bent, M. D. McGehee, *Nat. Energy* **2017**, *2*, 17009.

[157] X. Liu, N. Zhang, B. Tang, M. Li, Y. W. Zhang, Z. G. Yu, H. Gong, *J. Phys. Chem. Lett.* **2018**, *9*, 5862.

[158] Y. Dang, Y. Liu, Y. Sun, D. Yuan, X. Liu, W. Lu, G. Liu, H. Xia, X. Tao, *CrystEngComm* **2015**, *17*, 665.

[159] L. Dou, *J. Mater. Chem. C* **2017**, *5*, 11165.

[160] H. Zheng, G. Liu, X. Xu, A. Alsaedi, T. Hayat, X. Pan, S. Dai, *ChemSusChem* **2018**, *11*, 3269.

[161] H. Matsui, K. Okada, T. Kitamura, N. Tanabe, *Sol. Energy Mater. Sol. Cells* **2009**, *93*, 1110.

[162] S. A. Gevorgyan, A. J. Medford, E. Bundgaard, S. B. Sapkota, H.-F. Schleiermacher, B. Zimmermann, U. Würfel, A. Chafiq, M. Lira-Cantu, T. Swonke, M. Wagner, C. J. Brabec, O. Haillant, E. Voroshazi, T. Aernouts, R. Steim, J. A. Hauch, A. Elschner, M. Pannone, M. Xiao, A. Langzettel, D. Laird, M. T. Lloyd, T. Rath, E. Maier, G. Trimmel, M. Hermenau, T. Menke, K. Leo, R. Rösch, M. Seeland, H. Hoppe, T. J. Nagle, K. B. Burke, C. J. Fell, D. Vak, T. B. Singh, S. E. Watkins, Y. Galagan, A. Manor, E. A. Katz, T. Kim, K. Kim, P. M. Sommeling, W. J. H. Verhees, S. C. Veenstra, M. Riede, M. Greyson Christoforo, T. Currier, V. Shrotriya, G. Schwartz, F. C. Krebs, *Sol. Energy Mater. Sol. Cells* **2011**, *95*, 1398.
[163] a) R. Roesch, T. Faber, E. von Hauff, T. M. Brown, M. Lira-Cantu, H. Hoppe, *Adv. Energy Mater.* **2015**, *5*, 1501407; b) A. Fakharuddin, F. Di Giacomo, A. L. Palma, F. Matteocci, I. Ahmed, S. Razza, A. D'Epifanio, S. Licoccia, J. Ismail, A. Di Carlo, T. M. Brown, R. Jose, *ACS Nano* **2015**, *9*, 8420.
[164] K. Leo, *Nat. Nanotechnol.* **2015**, *10*, 574.
[165] M. Kulbak, D. Cahen, G. Hodes, *J. Phys. Chem. Lett.* **2015**, *6*, 2452.
[166] H. Choi, J. Jeong, H.-B. Kim, S. Kim, B. Walker, G.-H. Kim, J. Y. Kim, *Nano Energy* **2014**, *7*, 80.
[167] C. C. Stoumpos, C. D. Malliakas, M. G. Kanatzidis, *Inorg. Chem.* **2013**, *52*, 9019.
[168] V. Goldschmidt, S. Videnskaps-Akad, I. Oslo, *Mat. Nat. Kl8* **1926**.
[169] A. Amat, E. Mosconi, E. Ronca, C. Quarti, P. Umari, M. K. Nazeeruddin, M. Gratzel, F. De Angelis, *Nano Lett.* **2014**, *14*, 3608.
[170] a) C. C. Stoumpos, M. G. Kanatzidis, *Acc. Chem. Res.* **2015**, *48*, 2791; b) G. Kieslich, S. Sun, A. K. Cheetham, *Chem. Sci.* **2014**, *5*, 4712.
[171] A. Poglitsch, D. Weber, *J. Chem. Phys.* **1987**, *87*, 6373.
[172] G. E. Eperon, S. D. Stranks, C. Menelaou, M. B. Johnston, L. M. Herz, H. J. Snaith, *Energy Environ. Sci.* **2014**, *7*, 982.
[173] J. Xue, J.-W. Lee, Z. Dai, R. Wang, S. Nuryyeva, M. E. Liao, S.-Y. Chang, L. Meng, D. Meng, P. Sun, O. Lin, M. S. Goorsky, Y. Yang, *Joule* **2018**, *2*, 1866.
[174] M. Saliba, T. Matsui, K. Domanski, J. Y. Seo, A. Ummadisingu, S. M. Zakeeruddin, J. P. Correa-Baena, W. R. Tress, A. Abate, A. Hagfeldt, M. Gratzel, *Science* **2016**, *354*, 206.
[175] G. Liu, H. Zheng, X. Xu, L.-Z. Zhu, X. Zhang, X. Pan, *Chem. Mater.* **2018**, *30*, 7691.
[176] L. N. Quan, M. Yuan, R. Comin, O. Voznyy, E. M. Beauregard, S. Hoogland, A. Buin, A. R. Kirmani, K. Zhao, A. Amassian, D. H. Kim, E. H. Sargent, *J. Am. Chem. Soc.* **2016**, *138*, 2649.
[177] K. Yamamoto, S. Iikubo, J. Yamasaki, Y. Ogomi, S. Hayase, *J. Phys. Chem. C* **2017**, *121*, 27797.
[178] M. R. Filip, G. E. Eperon, H. J. Snaith, F. Giustino, *Nat. Commun.* **2014**, *5*, 5757.
[179] L. Fu, Y. Zhang, B. Chang, B. Li, S. Zhou, L. Zhang, L. Yin, *J. Mater. Chem. A* **2018**, *6*, 13263.
[180] a) C. Bernal, K. Yang, *J. Phys. Chem. C* **2014**, *118*, 24383; b) P. Xu, S. Chen, H.-J. Xiang, X.-G. Gong, S.-H. Wei, *Chem. Mater.* **2014**, *26*, 6068; c) T. J. Jacobsson, M. Pazoki, A. Hagfeldt, T. Edvinsson, *J. Phys. Chem. C* **2015**, *119*, 25673; d) Y. Y. Sun, J. Shi, J. Lian, W. Gao, M. L. Agiorgousis, P. Zhang, S. Zhang, *Nanoscale* **2016**, *8*, 6284.
[181] Y. Wang, J. Cheng, M. Behtash, W. Tang, J. Luo, K. Yang, *Phys. Chem. Chem. Phys.* **2018**, *20*, 18515.
[182] D. P. McMeekin, G. Sadoughi, W. Rehman, G. E. Eperon, M. Saliba, M. T. Horantner, A. Haghighirad, N. Sakai, L. Korte, B. Rech, M. B. Johnston, L. M. Herz, H. J. Snaith, *Science* **2016**, *351*, 151.
[183] S. N. Marshenya, B. V. Politov, A. Y. Suntsov, I. A. Leonidov, S. A. Petrova, M. V. Patrakeev, V. L. Kozhevnikov, *J. Alloys Compd.* **2018**, *767*, 1041.
[184] E. Bi, H. Chen, F. Xie, Y. Wu, W. Chen, Y. Su, A. Islam, M. Gratzel, X. Yang, L. Han, *Nat. Commun.* **2017**, *8*, 15330.
[185] L. Liu, S. Huang, Y. Lu, P. Liu, Y. Zhao, C. Shi, S. Zhang, J. Wu, H. Zhong, M. Sui, H. Zhou, H. Jin, Y. Li, Q. Chen, *Adv. Mater.* **2018**, *30*, 1800544.
[186] Z. Li, C. Xiao, Y. Yang, S. P. Harvey, D. H. Kim, J. A. Christians, M. Yang, P. Schulz, S. U. Nanayakkara, C.-S. Jiang, J. M. Luther, J. J. Berry, M. C. Beard, M. M. Al-Jassim, K. Zhu, *Energy Environ. Sci.* **2017**, *10*, 1234.
[187] L.-L. Jiang, Z.-K. Wang, M. Li, C.-C. Zhang, Q.-Q. Ye, K.-H. Hu, D.-Z. Lu, P.-F. Fang, L.-S. Liao, *Adv. Funct. Mater.* **2018**, *28*, 1705875.
[188] J. W. Lee, Z. Dai, T. H. Han, C. Choi, S. Y. Chang, S. J. Lee, N. De Marco, H. Zhao, P. Sun, Y. Huang, Y. Yang, *Nat. Commun.* **2018**, *9*, 3021.
[189] a) F. Xia, Q. Wu, P. Zhou, Y. Li, X. Chen, Q. Liu, J. Zhu, S. Dai, Y. Lu, S. Yang, *ACS Appl. Mater. Interfaces* **2015**, *7*, 13659; b) A. Bera, A. D. Sheikh, M. A. Haque, R. Bose, E. Alarousu, O. F. Mohammed, T. Wu, *ACS Appl. Mater. Interfaces* **2015**, *7*, 28404.
[190] J. Lian, B. Lu, F. Niu, P. Zeng, X. Zhan, *Small Methods* **2018**, *2*, 1800082.
[191] L. Zhu, J. Ye, X. Zhang, H. Zheng, G. Liu, X. Pan, S. Dai, *J. Mater. Chem. A* **2017**, *5*, 3675.
[192] Y. Shao, Z. Xiao, C. Bi, Y. Yuan, J. Huang, *Nat. Commun.* **2014**, *5*, 5784.
[193] a) H. S. Kim, J. W. Lee, N. Yantara, P. P. Boix, S. A. Kulkarni, S. Mhaisalkar, M. Gratzel, N. G. Park, *Nano Lett.* **2013**, *13*, 2412; b) W. Ke, G. Fang, Q. Liu, L. Xiong, P. Qin, H. Tao, J. Wang, H. Lei, B. Li, J. Wan, G. Yang, Y. Yan, *J. Am. Chem. Soc.* **2015**, *137*, 6730.
[194] C. Chen, Y. Cheng, Q. Dai, H. Song, *Sci. Rep.* **2015**, *5*, 17684.
[195] W. Qiu, U. W. Paetzold, R. Gehlhaar, V. Smirnov, H.-G. Boyen, J. G. Tait, B. Conings, W. Zhang, C. B. Nielsen, I. McCulloch, L. Froyen, P. Heremans, D. Cheyns, *J. Mater. Chem. A* **2015**, *3*, 22824.
[196] W. Ke, G. Fang, J. Wang, P. Qin, H. Tao, H. Lei, Q. Liu, X. Dai, X. Zhao, *ACS Appl. Mater. Interfaces* **2014**, *6*, 15959.
[197] H. Wang, Y. Liu, H. Liu, Z. Chen, P. Xiong, X. Xu, F. Chen, K. Li, Y. Duan, *Adv. Mater. Interfaces* **2018**, *5*, 1701248.
[198] J.-Y. Seo, R. Uchida, H.-S. Kim, Y. Saygili, J. Luo, C. Moore, J. Kerrod, A. Wagstaff, M. Eklund, R. McIntyre, N. Pellet, S. M. Zakeeruddin, A. Hagfeldt, M. Grätzel, *Adv. Funct. Mater.* **2018**, *28*, 1705763.
[199] J. Qiu, Y. Qiu, K. Yan, M. Zhong, C. Mu, H. Yan, S. Yang, *Nanoscale* **2013**, *5*, 3245.
[200] Q. Zhang, C. S. Dandeneau, X. Zhou, G. Cao, *Adv. Mater.* **2009**, *21*, 4087.
[201] F. J. Ramos, M. C. Lopez-Santos, E. Guillen, M. K. Nazeeruddin, M. Gratzel, A. R. Gonzalez-Elipe, S. Ahmad, *ChemPhysChem* **2014**, *15*, 1148.
[202] P. Zhang, J. Wu, T. Zhang, Y. Wang, D. Liu, H. Chen, L. Ji, C. Liu, W. Ahmad, Z. D. Chen, S. Li, *Adv. Mater.* **2018**, *30*, 1703737.
[203] D. Bi, G. Boschloo, S. Schwarzmuller, L. Yang, E. M. Johansson, A. Hagfeldt, *Nanoscale* **2013**, *5*, 11686.
[204] K. Mahmood, B. S. Swain, A. Amassian, *Adv. Energy Mater.* **2015**, *5*, 1500568.
[205] D. Liu, T. L. Kelly, *Nat. Photonics* **2013**, *8*, 133.
[206] J. Zhang, P. Barboux, T. Pauporté, *Adv. Energy Mater.* **2014**, *4*, 1400932.
[207] Z.-L. Tseng, C.-H. Chiang, S.-H. Chang, C.-G. Wu, *Nano Energy* **2016**, *28*, 311.
[208] S. Song, G. Kang, L. Pyeon, C. Lim, G.-Y. Lee, T. Park, J. Choi, *ACS Energy Lett.* **2017**, *2*, 2667.
[209] J. Song, E. Zheng, J. Bian, X.-F. Wang, W. Tian, Y. Sanehira, T. Miyasaka, *J. Mater. Chem. A* **2015**, *3*, 10837.

[210] Y. Kuang, V. Zardetto, R. van Gils, S. Karwal, D. Koushik, M. A. Verheijen, L. E. Black, C. Weijtens, S. Veenstra, R. Andriessen, W. M. M. Kessels, M. Creatore, *ACS Appl. Mater. Interfaces* **2018**, *10*, 30367.
[211] M. Hou, H. Zhang, Z. Wang, Y. Xia, Y. Chen, W. Huang, *ACS Appl. Mater. Interfaces* **2018**, *10*, 30607.
[212] D. Liu, J. Yang, T. L. Kelly, *J. Am. Chem. Soc.* **2014**, *136*, 17116.
[213] Z. Zhu, Y. Bai, X. Liu, C. C. Chueh, S. Yang, A. K. Jen, *Adv. Mater.* **2016**, *28*, 6478.
[214] C.-Z. Li, C.-C. Chueh, H.-L. Yip, J. Zou, W.-C. Chen, A. K. Y. Jen, *J. Mater. Chem.* **2012**, *22*, 14976.
[215] C. A. Reed, R. D. Bolskar, *Chem. Rev.* **2000**, *100*, 1075.
[216] Y. Fang, C. Bi, D. Wang, J. Huang, *ACS Energy Lett.* **2017**, *2*, 782.
[217] S. Pfuetzner, J. Meiss, A. Petrich, M. Riede, K. Leo, *Appl. Phys. Lett.* **2009**, *94*, 223307.
[218] H. Yoon, S. M. Kang, J.-K. Lee, M. Choi, *Energy Environ. Sci.* **2016**, *9*, 2262.
[219] X. Meng, Y. Bai, S. Xiao, T. Zhang, C. Hu, Y. Yang, X. Zheng, S. Yang, *Nano Energy* **2016**, *30*, 341.
[220] C. Tian, K. Kochiss, E. Castro, G. Betancourt-Solis, H. Han, L. Echegoyen, *J. Mater. Chem. A* **2017**, *5*, 7326.
[221] S.-K. Jung, J. H. Heo, D. W. Lee, S.-C. Lee, S.-H. Lee, W. Yoon, H. Yun, S. H. Im, J. H. Kim, O. P. Kwon, *Adv. Funct. Mater.* **2018**, *28*, 1800346.
[222] X. Liu, C.-C. Chueh, Z. Zhu, S. B. Jo, Y. Sun, A. K. Y. Jen, *J. Mater. Chem. A* **2016**, *4*, 15294.
[223] S. M. Yang, H. Z. Kou, J. C. Wang, H. B. Xue, H. L. Han, *J. Phys. Chem. C* **2010**, *114*, 4245.
[224] D.-B. Li, L. Hu, Y. Xie, G. Niu, T. Liu, Y. Zhou, L. Gao, B. Yang, J. Tang, *ACS Photonics* **2016**, *3*, 2122.
[225] S. S. Shin, E. J. Yeom, W. S. Yang, S. Hur, M. G. Kim, J. Im, J. Seo, J. H. Noh, S. I. Seok, *Science* **2017**, *356*, 167.
[226] A. Krishna, A. C. Grimsdale, *J. Mater. Chem. A* **2017**, *5*, 16446.
[227] G.-W. Kim, G. Kang, M. Malekshahi Byranvand, G.-Y. Lee, T. Park, *ACS Appl. Mater. Interfaces* **2017**, *9*, 27720.
[228] L. Wagner, S. Chacko, G. Mathiazhagan, S. Mastroianni, A. Hinsch, *ACS Energy Lett.* **2018**, *3*, 1122.
[229] A. T. Barrows, A. J. Pearson, C. K. Kwak, A. D. F. Dunbar, A. R. Buckley, D. G. Lidzey, *Energy Environ. Sci.* **2014**, *7*, 2944.
[230] J. Lian, Q. Wang, Y. Yuan, Y. Shao, J. Huang, *J. Mater. Chem. A* **2015**, *3*, 9146.
[231] L. Hu, M. Li, K. Yang, Z. Xiong, B. Yang, M. Wang, X. Tang, Z. Zang, X. Liu, B. Li, Z. Xiao, S. Lu, H. Gong, J. Ouyang, K. Sun, *J. Mater. Chem. A* **2018**, *6*, 16583.
[232] B. Wang, Z.-G. Zhang, S. Ye, H. Rao, Z. Bian, C. Huang, Y. Li, *J. Mater. Chem. A* **2016**, *4*, 17267.
[233] Z. K. Wang, X. Gong, M. Li, Y. Hu, J. M. Wang, H. Ma, L. S. Liao, *ACS Nano* **2016**, *10*, 5479.
[234] S. Shao, J. Liu, J. Bergqvist, S. Shi, C. Veit, U. Würfel, Z. Xie, F. Zhang, *Adv. Energy Mater.* **2013**, *3*, 349.
[235] F. Hou, Z. Su, F. Jin, X. Yan, L. Wang, H. Zhao, J. Zhu, B. Chu, W. Li, *Nanoscale* **2015**, *7*, 9427.
[236] Z. Hawash, L. K. Ono, Y. Qi, *Adv. Mater. Interfaces* **2018**, *5*, 1700623.
[237] Q. Luo, Y. Zhang, C. Liu, J. Li, N. Wang, H. Lin, *J. Mater. Chem. A* **2015**, *3*, 15996.
[238] M. A. Green, A. Ho-Baillie, H. J. Snaith, *Nat. Photonics* **2014**, *8*, 506.
[239] K. Domanski, J. P. Correa-Baena, N. Mine, M. K. Nazeeruddin, A. Abate, M. Saliba, W. Tress, A. Hagfeldt, M. Gratzel, *ACS Nano* **2016**, *10*, 6306.
[240] M. A. Green, K. Emery, Y. Hishikawa, W. Warta, E. D. Dunlop, *Prog. Photovoltaics* **2016**, *24*, 905.
[241] M. Ye, X. Hong, F. Zhang, X. Liu, *J. Mater. Chem. A* **2016**, *4*, 6755.
[242] T.-T. Bui, M. Ulfa, F. Maschietto, A. Ottochian, M.-P. Nghiêm, I. Ciofini, F. Goubard, T. Pauporté, *Org. Electron.* **2018**, *60*, 22.
[243] Y. Yue, N. Salim, Y. Wu, X. Yang, A. Islam, W. Chen, J. Liu, E. Bi, F. Xie, M. Cai, L. Han, *Adv. Mater.* **2016**, *28*, 10738.
[244] J. Zhang, T. Zhang, L. Jiang, U. Bach, Y.-B. Cheng, *ACS Energy Lett.* **2018**, *3*, 1677.
[245] S. S. Mali, H. Kim, J. V. Patil, C. K. Hong, *ACS Appl. Mater. Interfaces* **2018**, *10*, 31280.
[246] Q. Wang, C. Bi, J. S. Huang, *Nano Energy* **2015**, *15*, 275.
[247] Z. P. Wang, Q. Q. Lin, B. Wenger, M. G. Christoforo, Y. H. Lin, M. T. Klug, M. B. Johnston, L. M. Herz, H. J. Snaith, *Nat. Energy* **2018**, *3*, 855.
[248] a) M.-H. Li, P.-S. Shen, K.-C. Wang, T.-F. Guo, P. Chen, *J. Mater. Chem. A* **2015**, *3*, 9011; b) J. Y. Jeng, K. C. Chen, T. Y. Chiang, P. Y. Lin, T. D. Tsai, Y. C. Chang, T. F. Guo, P. Chen, T. C. Wen, Y. J. Hsu, *Adv. Mater.* **2014**, *26*, 4107.
[249] X. Yin, J. Zhai, T. Wang, W. Jing, L. Song, J. Xiong, *Mater. Lett.* **2018**, *231*, 101.
[250] Q. Guo, C. Wang, J. Li, Y. Bai, F. Wang, L. Liu, B. Zhang, T. Hayat, A. Alsaedi, Z. Tan, *Phys. Chem. Chem. Phys.* **2018**, *20*, 21746.
[251] C. Duan, M. Zhao, C. Zhao, Y. Wang, J. Li, W. Han, Q. Hu, L. Yao, H. Jian, F. Lu, T. Jiu, *Mater. Today Energy* **2018**, *9*, 487.
[252] D. Han, C. Wu, Q. Zhang, S. Wei, X. Qi, Y. Zhao, Y. Chen, Y. Chen, L. Xiao, Z. Zhao, *ACS Appl. Mater. Interfaces* **2018**, *10*, 31535.
[253] G.-W. Kim, G. Kang, K. Choi, H. Choi, T. Park, *Adv. Energy Mater.* **2018**, *8*, 1801386.
[254] K. Mahmood, S. Sarwar, M. T. Mehran, *RSC Adv.* **2017**, *7*, 17044.
[255] Y. Kato, L. K. Ono, M. V. Lee, S. Wang, S. R. Raga, Y. Qi, *Adv. Mater. Interfaces* **2015**, *2*, 1500195.
[256] J. Wang, X. Chen, F. Jiang, Q. Luo, L. Zhang, M. Tan, M. Xie, Y.-Q. Li, Y. Zhou, W. Su, Y. Li, C.-Q. Ma, *Sol. RRL* **2018**, *2*, 1800118.
[257] S. Seo, S. Jeong, C. Bae, N. G. Park, H. Shin, *Adv. Mater.* **2018**, *30*, 1801010.
[258] A. Guerrero, J. You, C. Aranda, Y. S. Kang, G. Garcia-Belmonte, H. Zhou, J. Bisquert, Y. Yang, *ACS Nano* **2016**, *10*, 218.
[259] H. Back, G. Kim, J. Kim, J. Kong, T. K. Kim, H. Kang, H. Kim, J. Lee, S. Lee, K. Lee, *Energy Environ. Sci.* **2016**, *9*, 1258.
[260] Y. Han, S. Meyer, Y. Dkhissi, K. Weber, J. M. Pringle, U. Bach, L. Spiccia, Y.-B. Cheng, *J. Mater. Chem. A* **2015**, *3*, 8139.
[261] T. Y. Yang, G. Gregori, N. Pellet, M. Gratzel, J. Maier, *Angew. Chem., Int. Ed. Engl.* **2015**, *54*, 7905.
[262] J. T. Tisdale, E. Muckley, M. Ahmadi, T. Smith, C. Seal, E. Lukosi, I. N. Ivanov, B. Hu, *Adv. Mater. Interfaces* **2018**, *5*, 1800476.
[263] J. H. Park, J. Seo, S. Park, S. S. Shin, Y. C. Kim, N. J. Jeon, H. W. Shin, T. K. Ahn, J. H. Noh, S. C. Yoon, C. S. Hwang, S. I. Seok, *Adv. Mater.* **2015**, *27*, 4013.
[264] J. Zhao, X. Zheng, Y. Deng, T. Li, Y. Shao, A. Gruverman, J. Shield, J. Huang, *Energy Environ. Sci.* **2016**, *9*, 3650.
[265] F. Guo, H. Azimi, Y. Hou, T. Przybilla, M. Hu, C. Bronnbauer, S. Langner, E. Spiecker, K. Forberich, C. J. Brabec, *Nanoscale* **2015**, *7*, 1642.
[266] X. Dai, Y. Zhang, H. Shen, Q. Luo, X. Zhao, J. Li, H. Lin, *ACS Appl. Mater. Interfaces* **2016**, *8*, 4523.
[267] a) M. Kaltenbrunner, G. Adam, E. D. Glowacki, M. Drack, R. Schwodiauer, L. Leonat, D. H. Apaydin, H. Groiss, M. C. Scharber, M. S. White, N. S. Sariciftci, S. Bauer, *Nat. Mater.* **2015**, *14*, 1032; b) E. M. Sanehira, B. J. Tremolet de Villers, P. Schulz, M. O. Reese, S. Ferrere, K. Zhu, L. Y. Lin, J. J. Berry, J. M. Luther, *ACS Energy Lett.* **2016**, *1*, 38.
[268] W.-C. Lai, K.-W. Lin, T.-F. Guo, P. Chen, Y.-Y. Liao, *Appl. Phys. Lett.* **2018**, *112*, 071103.
[269] A. Agresti, S. Pescetelli, L. Cinà, D. Konios, G. Kakavelakis, E. Kymakis, A. D. Carlo, *Adv. Funct. Mater.* **2016**, *26*, 2686.
[270] a) S. Guarnera, A. Abate, W. Zhang, J. M. Foster, G. Richardson, A. Petrozza, H. J. Snaith, *J. Phys. Chem. Lett.* **2015**, *6*, 432; b) D. Yu, Y. Q. Yang, Z. Chen, Y. Tao, Y. F. Liu, *Opt. Commun.* **2016**, *362*, 43.

[271] Y. Duan, X. Wang, Y. H. Duan, Y. Q. Yang, P. Chen, D. Yang, F. B. Sun, K. W. Xue, N. Hu, J. W. Hou, *Org. Electron.* **2014**, *15*, 1936.
[272] F. B. Sun, Y. Duan, Y. Q. Yang, P. Chen, Y. H. Duan, X. Wang, D. Yang, K. W. Xue, *Org. Electron.* **2014**, *15*, 2546.
[273] F. Liu, Q. Dong, M. K. Wong, A. B. Djurišić, A. Ng, Z. Ren, Q. Shen, C. Surya, W. K. Chan, J. Wang, A. M. C. Ng, C. Liao, H. Li, K. Shih, C. Wei, H. Su, J. Dai, *Adv. Energy Mater.* **2016**, *6*, 1502206.
[274] B. Li, Y. Li, C. Zheng, D. Gao, W. Huang, *RSC Adv.* **2016**, *6*, 38079.
[275] F. C. Krebs, S. A. Gevorgyan, J. Alstrup, *J. Mater. Chem.* **2009**, *19*, 5442.
[276] A. S. da Silva Sobrinho, M. Latrèche, G. Czeremuszkin, J. E. Klemberg-Sapieha, M. R. Wertheimer, *J. Vac. Sci. Technol., A* **1998**, *16*, 3190.
[277] N. Kim, W. J. Potscavage, A. Sundaramoothi, C. Henderson, B. Kippelen, S. Graham, *Sol. Energy Mater. Sol. Cells* **2012**, *101*, 140.
[278] J. Ahmad, K. Bazaka, L. J. Anderson, R. D. White, M. V. Jacob, *Renewable Sustainable Energy Rev.* **2013**, *27*, 104.
[279] F. J. Ramos, D. Cortes, A. Aguirre, F. I. Castano, S. Ahmad, *2014 IEEE 40th Photovoltaic Specialist Conf. (Pvsc)*, Vol. *2584*, IEEE, June **2014**, pp. 8–13.
[280] I. Hwang, I. Jeong, J. Lee, M. J. Ko, K. Yong, *ACS Appl. Mater. Interfaces* **2015**, *7*, 17330.
[281] C.-Y. Chang, K.-T. Lee, W.-K. Huang, H.-Y. Siao, Y.-C. Chang, *Chem. Mater.* **2015**, *27*, 5122.
[282] J. Idigoras, F. J. Aparicio, L. Contreras-Bernal, S. Ramos-Terron, M. Alcaire, J. R. Sanchez-Valencia, A. Borras, A. Barranco, J. A. Anta, *ACS Appl. Mater. Interfaces* **2018**, *10*, 11587.
[283] H. C. Weerasinghe, Y. Dkhissi, A. D. Scully, R. A. Caruso, Y.-B. Cheng, *Nano Energy* **2015**, *18*, 118.
[284] B. J. Kim, H. Park, H. Seong, M. S. Lee, B.-H. Kwon, D. H. Kim, Y. I. Lee, H. Lee, J.-I. Lee, S. G. Im, *Adv. Eng. Mater.* **2017**, *19*, 1600819.
[285] Y. I. Lee, N. J. Jeon, B. J. Kim, H. Shim, T.-Y. Yang, S. I. Seok, J. Seo, S. G. Im, *Adv. Energy Mater.* **2018**, *8*, 1701928.
[286] M. Lipiñsk, *Arch. Mater. Sci. Eng.* **2010**, *46*, 69.
[287] G. Dennler, C. Lungenschmied, H. Neugebauer, N. S. Sariciftci, M. Latrèche, G. Czeremuszkin, M. R. Wertheimer, *Thin Solid Films* **2006**, *511–512*, 349.
[288] E. Lay, D.-S. Wuu, S.-Y. Lo, R.-H. Horng, H.-F. Wei, L.-Y. Jiang, H.-U. Lee, Y.-Y. Chang, *Surf. Coat. Technol.* **2011**, *205*, 4267.
[289] W. J. Potscavage, S. Yoo, B. Domercq, B. Kippelen, *Appl. Phys. Lett.* **2007**, *90*, 253511.
[290] A. A. Dameron, S. D. Davidson, B. B. Burton, P. F. Carcia, R. S. McLean, S. M. George, *J. Phys. Chem. C* **2008**, *112*, 4573.
[291] a) J. Schlothauer, S. Jungwirth, M. Köhl, B. Röder, *Sol. Energy Mater. Sol. Cells* **2012**, *102*, 75; b) J. Jin, S. Chen, J. Zhang, *J. Polym. Res.* **2009**, *17*, 827.
[292] E. Cuddihy, C. Coulbert, A. Gupta, R. Liang, *U.S. Department of Energy's National Photovoltaics Program* **1986**, http://resolver.caltech.edu/JPLpub86-31-volumeVII 02/06/2019.
[293] J. Yin, H. Zhu, Y. Wang, Z. Wang, J. Gao, Y. Mai, Y. Ma, M. Wan, Y. Huang, *Appl. Surf. Sci.* **2012**, *259*, 758.
[294] a) G. Rowell, *PhD Thesis*, University of California **2009**; b) Z. Chen, H. Wang, X. Wang, P. Chen, Y. Liu, H. Zhao, Y. Zhao, Y. Duan, *Sci. Rep.* **2017**, *7*, 40061.
[295] H. Heuer, C. Wenzel, D. Herrmann, R. Hübner, Z. L. Zhang, J. W. Bartha, *Thin Solid Films* **2006**, *515*, 1612.
[296] T. J. Wilderspin, F. De Rossi, T. M. Watson, *Sol. Energy* **2016**, *139*, 426.
[297] K. P. Bhandari, J. M. Collier, R. J. Ellingson, D. S. Apul, *Renewable Sustainable Energy Rev.* **2015**, *47*, 133.
[298] A. Bhat, B. Dhamaniya, P. Chhillar, T. Korukonda, G. Rawat, S. Pathak, *Crystals* **2018**, *8*, 242.
[299] A. A. Asif, R. Singh, G. F. Alapatt, *J. Renewable Sustainable Energy* **2015**, *7*, 043120.
[300] N.-G. Park, M. Grätzel, T. Miyasaka, K. Zhu, K. Emery, *Nat. Energy* **2016**, *1*, 16152.
[301] B. Hailegnaw, S. Kirmayer, E. Edri, G. Hodes, D. Cahen, *J. Phys. Chem. Lett.* **2015**, *6*, 1543.
[302] J. Gong, S. B. Darling, F. You, *Energy Environ. Sci.* **2015**, *8*, 1953.
[303] U. S. E. I. Administration, *Resources in the Annual Energy Outlook 2018*, **2018**, https://www.eia.gov/outlooks/aeo/ (accessed: February 2019).
[304] T. Leijtens, G. E. Eperon, N. K. Noel, S. N. Habisreutinger, A. Petrozza, H. J. Snaith, *Adv. Energy Mater.* **2015**, *5*, 1500963.
[305] A. Binek, M. L. Petrus, N. Huber, H. Bristow, Y. Hu, T. Bein, P. Docampo, *ACS Appl. Mater. Interfaces* **2016**, *8*, 12881.
[306] N. L. Chang, A. W. Yi Ho-Baillie, P. A. Basore, T. L. Young, R. Evans, R. J. Egan, *Prog. Photovoltaics* **2017**, *25*, 390.
[307] W. Zhu, C. Bao, F. Li, T. Yu, H. Gao, Y. Yi, J. Yang, G. Fu, X. Zhou, Z. Zou, *Nano Energy* **2016**, *19*, 17.
[308] W. Huang, J. S. Manser, P. V. Kamat, S. Ptasinska, *Chem. Mater.* **2015**, *28*, 303.
[309] S. Shao, Z. Chen, H. H. Fang, G. H. ten Brink, D. Bartesaghi, S. Adjokatse, L. J. A. Koster, B. J. Kooi, A. Facchetti, M. A. Loi, *J. Mater. Chem. A* **2016**, *4*, 2419.
[310] B. Suarez, V. Gonzalez-Pedro, T. S. Ripolles, R. S. Sanchez, L. Otero, I. Mora-Sero, *J. Phys. Chem. Lett.* **2014**, *5*, 1628.
[311] Q. Tai, P. You, H. Sang, Z. Liu, C. Hu, H. L. Chan, F. Yan, *Nat. Commun.* **2016**, *7*, 11105.
[312] J. Barbe, M. L. Tietze, M. Neophytou, B. Murali, E. Alarousu, A. E. Labban, M. Abulikemu, W. Yue, O. F. Mohammed, I. McCulloch, A. Amassian, S. Del Gobbo, *ACS Appl. Mater. Interfaces* **2017**, *9*, 11828.
[313] W. Yu, F. Li, H. Wang, E. Alarousu, Y. Chen, B. Lin, L. Wang, M. N. Hedhili, Y. Li, K. Wu, X. Wang, O. F. Mohammed, T. Wu, *Nanoscale* **2016**, *8*, 6173.
[314] B. A. Nejand, V. Ahmadi, H. R. Shahverdi, *ACS Appl. Mater. Interfaces* **2015**, *7*, 21807.
[315] M. Higgins, F. Ely, R. C. Nome, R. A. Nome, D. P. dos Santos, H. Choi, S. Nam, M. Quevedo-Lopez, *J. Appl. Phys.* **2018**, *124*, 065306.
[316] S. Li, H. Zhang, W. Zhao, L. Ye, H. Yao, B. Yang, S. Zhang, J. Hou, *Adv. Energy Mater.* **2016**, *6*, 1501991.
[317] H. Zheng, G. Liu, C. Zhang, L. Zhu, A. Alsaedi, T. Hayat, X. Pan, S. Dai, *Sol. Energy* **2018**, *159*, 914.
[318] C. S. Ponseca Jr., P. Chabera, J. Uhlig, P. Persson, V. Sundstrom, *Chem. Rev.* **2017**, *117*, 10940.
[319] K. Wojciechowski, T. Leijtens, S. Siprova, C. Schlueter, M. T. Horantner, J. T. Wang, C. Z. Li, A. K. Jen, T. L. Lee, H. J. Snaith, *J. Phys. Chem. Lett.* **2015**, *6*, 2399.
[320] F. Bella, G. Griffini, J. P. Correa-Baena, G. Saracco, M. Gratzel, A. Hagfeldt, S. Turri, C. Gerbaldi, *Science* **2016**, *354*, 203.
[321] H. Tsai, R. Asadpour, J. C. Blancon, C. C. Stoumpos, O. Durand, J. W. Strzalka, B. Chen, R. Verduzco, P. M. Ajayan, S. Tretiak, J. Even, M. A. Alam, M. G. Kanatzidis, W. Nie, A. D. Mohite, *Science* **2018**, *360*, 67.
[322] H. Chen, F. Ye, W. Tang, J. He, M. Yin, Y. Wang, F. Xie, E. Bi, X. Yang, M. Gratzel, L. Han, *Nature* **2017**, *550*, 92.